Norges miljø- og
biovitenskapelige
universitet

Master's Thesis 2016 60 ECTS
Department of Chemistry, Biotechnology and Food Science

Characterization of Cytostatic Drug Responses and Signaling Aberrations in Chronic Lymphocytic Leukemia

Ida K. Myhrvold

Characterization of Cytostatic Drug Responses and Signaling Aberrations in Chronic Lymphocytic Leukemia

Author

Ida K. Myhrvold

Main supervisor

Professor Dr. med. Kjetil Taskén

Co-supervisor

Researcher Dr. Sigrid S. Skånland

Main Supervisor (NMBU)

Professor Tor Lea

Norwegian University of Life Sciences

Acknowledgments

The work presented in this master thesis was performed at the Norwegian Center for Molecular Medicine (NCMM), University of Oslo, in the group of Professor Dr. med. Kjetil Taskén and co-supervised by Dr. Sigrid S. Skånland. My internal supervisor at the Norwegian University of Life Sciences (NMBU), at the institute of Chemistry, Biotechnology and Food Science was Professor Tor Lea.

Professor Dr. med. Geir E. Tjønnfjord at the Department of Haematology, Oslo University Hospital, Rikshospitalet, provided patients samples as well as information about the patients and drugs in current use for CLL. Professor Dr. med. Ludvig A. Munthe and B.Sc. Sowmya Subbanna at the Centre for Immune regulation, Department of Immunology, Oslo University Hospital, Rikshospitalet, provided purified patients samples and collaborated on the experiment shown in Figure 11.

I would like to thank Kjetil Taskén and Sigrid S. Skånland for giving me the opportunity to be a part of this exciting project. Kjetil, thank you for your support and guidance throughout the lab-meetings and all feedback and input during the writing. Sigrid, you have always been available for all kind of questions and thanks a lot for all the help regarding practical lab work and great feedback and input during the writing. Professor Tor Lea, thanks for the feedback and input the last months and for taking care of the practical work regarding the exam.

Finally, I want to thank everyone in the Taskén group for all support and for an enjoyable working environment, especially Dr. Vanessa L. Wehbi.

Oslo, May, 2016

Ida K. Myhrvold

Sammendrag

Kronisk lymfatisk leukemi (KLL) er en heterogen sykdom med variabelt klinisk sykdomforløp. Det finnes i dag ingen helbredende behandling. For én tredjedel til halvparten av pasientene vil det aldri være nødvendig med behandling, men for de som trenger det, er tilbudet begrenset. I tillegg er forekomsten av KLL kraftig økende og det er dermed stigende etterspørselen etter et behandlingstilbud utover annenlinjebehandling. Arbeidet presentert i denne oppgaven er del av et større prosjekt hvor det langsiktige målet er å skreddersy behandlingen av KLL pasienter på et individuelt nivå. Som bidrag til dette har fosfovæskestrømscytometri blitt etablert i laben som metode for å analysere proteinfosforylering i B celler fra KLL pasienter og friske donorer. Ved hjelp av denne metoden har basal og indusert fosforylering i KLL og friske B celler blitt sammenlignet for å kartlegge avvik som kan indikere mål for terapi. Videre ble de cytostatiske medikamentene fludarabin, doksorubicin og vinkristin studert for å karakterisere deres effekt på basal og indusert fosforylering. Disse medikamentene er i bruk ved behandling av KLL og vil senere bli brukt i kombinasjonsstudier for screening av legemidler.

Studiet viste lavere basalt nivå av fosforyleringen av visse signalproteiner i B celler fra KLL pasienter relativt til friske donorer. Generelt ble denne effekten reversert av de cytostatiske medikamentene. STAT3 ($pTyr^{705}$), kjent for å være assosiert med hematologiske kreftformer, var oppregulert i KLL celler sammenlignet med kontrollceller. Etter BCR stimulering med anti-IgM og behandling med fludarabin eller doksorubicin, var det en økning av Akt ($pSer^{473}$) og p44/42 MAPK ($pThr^{202}/Tyr^{204}$) i KLL celler sammenlignet med friske kontroller. Den observerte effekten av fludarabin på Akt ($pSer^{473}$) ble kraftig reversert ved bruk av PI3K hemmeren idelalisib. Til slutt ble CD40 signalering undersøkt. CD40 stimulering resulterte i en økning av Akt ($pSer^{473}$) og i kombinasjon med fludarabin, doksorubicin eller vinkristin, viste en rekke parametre økt fosforylering.

Arbeidet presentert i denne oppgaven har ved bruk av fosfovæskestrømscytometri bidratt til å kartlegge basal, anti-IgM- og CD40L-indusert proteinfosforylering i KLL celler sammenlignet med friske B celler. Videre har det bidratt til viktig kunnskap om de effekter fludarabin, doksorubicin og vinkristin har på proteinfosforylering. Disse funnene vil være viktige i det videre arbeidet med å utvikle skreddersydd behandling av KLL pasienter.

Abstract

Chronic Lymphocytic Leukemia (CLL) is a heterogeneous disease with variable clinical courses. The disease is incurable, but a third to half of the patients may never need treatment. For those who need treatment, the options are limited and it is important to prevent them from exposure to ineffective therapy. The work presented in this master thesis is part of a larger project where the long-term goal is to tailor the treatment of CLL patients on an individual basis according to patients' biology and prognosis. The contributions to this goal were to establish phosphoflow cytometry as a method to analyse phosphorylation events in B cells from CLL patients and healthy donors in the lab. Applying this method, basal and induced phosphorylation levels in CLL cells relative to healthy controls were investigated in order to map aberrations which can provide indications for targeted therapy. The effects of the cytostatic drugs fludarabine, doxorubicin and vincristine on basal and induced levels of phosphorylation were also investigated.

The study showed that B cells from CLL patients exerted lower basal levels of phosphorylation of certain proteins relative to healthy controls. In general, the cytostatic drugs reversed this effect. Interestingly, STAT3 ($pTyr^{705}$) known to be associated with hematological malignancies, was upregulated in CLL cells compared to healthy controls. After BCR stimulation with anti-IgM, and fludarabine or doxorubicin treatment, Akt ($pSer^{473}$) and p44/42 MAPK ($pThr^{202}/Tyr^{204}$) were enhanced in CLL samples relative to healthy controls. Importantly, the PI3K inhibitor idelalisib potently reversed the effect of fludarabine on Akt ($pSer^{473}$). Finally, CD40 signaling was investigated, presenting a notable increase in Akt ($pSer^{473}$). In combination with fludarabine, doxorubicin or vincristine, the CD40L-induced phosphorylation was enhanced for several parameters. These drugs are currently in use for the treatment of CLL and will be used in combination studies in a future large-scale drug screen.

The work presented in this thesis has added to the mapping of basal, anti-IgM and CD40L-induced protein phosphorylation in CLL cells compared to healthy B cells by the use of phosphoflow cytometry analysis. Furthermore, it has provided important information on phosphorylation induced by the cytostatic drugs fludarabine, doxorubicin and vincristine. The findings reported here will be of value in the following studies which ultimately aim to provide personalized treatment of CLL patients.

Abbreviations

Akt/PKB - Protein kinase B
APC - Allophycocyanin
AP1 - Activator protein 1
ATP - Adenosine triphosphate
BCR - B cell receptor
BLNK - B cell linker protein
B cells - B lymphocytes
BCR - B cell receptor
Btk - Bruton's tyrosine kinase
BSA - bovine serum albumine
CAL-101/Idelalisib - 5-fluoro-3-phenyl-2-[(S)-1-(9H-purin-6-ylamino)-propyl]-3H-quinazolin-4-one
CD - Cluster of differentiation
$CD27^+$ - CD27 positive
CD40L - CD40 ligand
CLL - Chronic lymphocytic leukemia
CpG ODN - CpG-oligodeoxynucleotides
dCK - deoxycytidine kinase
DMSO - Dimethyl sulfoxide
DNA - Deoxyribonucleic acid
ERK1/2 - Extracellular signal-regulated kinase 1/2
Epo - Erythropoietin
FCB - Fluorescent cell barcoding
FCS - Fetal calf serum
FISH - Fluorescence *in situ* hybridisation
FITC - Fluorescein isothiocyanate
FSC - Forward scatter
GRB2 - Growth factor receptor-bound protein 2
IFNγ - Interferon γ
Ig - Immunoglobulin
IgHV - Immunoglobulin heavy chain variable region
IL-2 - Interleukin-2
ITAM - Immunoreceptor tyrosine-based activation motif
Itk - IL-2 inducible T cell kinase
iwCLL - international working group for CLL
JAK - Janus kinase
JNK - c-Jun N-terminal protein kinase
Lck - Lymphocyte-specific protein tyrosine kinase
MAPKAPK-2 - Mitogen activated protein kinase-activated protein kinase 2
MEK1 - Mitogen activated protein kinase kinase 1
M-CLL - Mutated CLL
mTOR - mammalian target of rapamycin
NK - Natural killer
NF-κB - Nuclear factor κ B
PBS - Phosphate-buffered saline
PKCβ - Protein kinase Cβ
PDK1 - Phosphoinositide-dependent protein kinase 1
PE - Phycoerythrin
PerCP-Cy5.5 - Peridinin chlorophyll protein Cyanine 5.5
PIP_2 - Phosphatidylinositol-4,5-bisphosphate
PIP_3 - Phosphatidylinositol-3,4,5-trisphosphate
PI3K - Phosphoinositide 3-kinase
PLCγ2 - Phospholipase C γ 2

p38 MAPK - p38 mitogen activated protein kinase
Raf - Raf proto-oncogene serine/threonine-protein kinase
Ras - Rat sarcoma protein
Rb - Retinoblastoma protein
RNA - Ribonucleic acid
SAPK - Stress activated protein kinase
sCD40L - soluble CD40 ligand
Ser - Serine
SH2 domain - Src homology 2domain
SLL - Small lymphocytic lymphoma
SOS - Son of sevenless
Src family kinase - Sarcoma family kinase
SSC - Side scatter
STAT - Signal transducer and activator of transcription
SYK - Spleen tyrosine kinase
S6-ribo prot - S6-ribosomal protein kinase
T cells - T lymphocytes
Thr - Threonine
Tyr - Tyrosine
TP53 - Tumor protein 53
UM-CLL - Unmutated CLL
ZAP70 - 70 kDa zeta-associated protein
p44/42 kDa MAPK - Mitogen activated protein kinase

Table of contents

1 Introduction 1

1.1 Chronic lymphocytic leukemia 1

1.1.1 Diagnosis of CLL 1

1.1.2 Staging of CLL 2

1.1.3 Biological markers of CLL and their prognostic impact 3

1.1.4 Treatment 6

1.2 Key signaling pathways in CLL 8

1.3 Phosphoflow cytometry 10

2 Objectives 13

3 Materials and Methods 15

3.1 Patient material and ethical considerations 15

3.2 Reagents and antibodies 15

3.3 Phosphoflow experiments 16

3.3.1 Purification of B lymphocytes from buffy coat 16

3.3.2 Stimulation and fixation 16

3.3.3 FCB 17

3.3.4 Antibody staining and phosphoflow cytometry analysis 17

3.3.5 Analysis in Cytobank 17

3.4 Stimulation and surface staining of B cells from CLL patients 17

4 Results 19

4.1 Impaired basal levels of phosphorylation in CLL cell samples relative to healthy controls 19

4.2 Elevated signaling in UM-CLL cells in response to anti-IgM stimulation 26

4.3 Fludarabine and doxorubicin enhance anti-IgM induced signaling 27

4.4 Idelalisib reverses the effect of fludarabine on Akt signaling 30

4.5 Increased activation of Akt in M-CLL cells upon sCD40L stimulation 31

4.6 Cytostatic drugs enhance sCD40L induced signaling 32

4.7 Fludarabine inhibits STAT1 signaling after IFNγ stimulation 34

5 Discussion 35

References 39

Supplement i

Total number of Supplementary Figures: 3

1 Introduction

Cancer refers to a large number of related diseases characterized by the development of abnormal cells that divide uncontrollably and have the ability to infiltrate and destroy normal body tissue (Cooper 2000). Cancer can develop almost anywhere in the body.

Leukemia is a type of cancer caused by distorted proliferation of abnormal white blood cells and their precursors in the blood and bone marrow. These abnormal blood cells are not able to fight infection and they occupy the bone marrow making less room for production of red blood cells and platelets (Pokharel 2012).

Leukemia can be divided into four main categories: Acute myelogenous leukemia (AML), Acute lymphocytic leukemia (ALL), Chronic myelogenous leukemia (CML) and Chronic lymphocytic leukemia (CLL). Acute leukemia progresses rapidly in contrast to chronic leukemia where the cells grow slowly. Myelogenous leukemia develops from myeloid cells which are the precursors for red blood cells, red platelets, mast cells, macrophages and granulocytes, whereas lymphocytic leukemia develops from lymphocytes (Pokharel 2012).

1.1 Chronic lymphocytic leukemia

Chronic Lymphocytic Leukemia (CLL) is a cancer characterized by accumulation of monoclonal, small mature B lymphocytes (B cells) in the blood, bone marrow and lymphoid tissue due to defective apoptosis (Dal-Bo et al. 2009; Watson et al. 2008). It is the most common form of leukemia in the Western world with about 200 and 15 000 new cases reported every year in Norway and USA, respectively (indicating incidences of 4 and 4,5 per 100 000 inhabitants, respectively) (Fabbri & Dalla-Favera 2016; Tjønnfjord et al. 2012). The median age at diagnosis is between 67-72 years, and males are affected more often than females. The relative risk for men is increasing with age, and at the age of 80, twice as many males are diagnosed compared to females (Watson et al. 2008).

1.1.1 Diagnosis of CLL

The guidelines for CLL diagnosis are provided by the international working group for CLL (iwCLL). One criterium is the presence of at least 5 x 10^9 B lymphocytes/L in peripheral blood persisting for more than 3 months. The expression of T lymphocyte (T cell) antigen CD5 and B-cell surface antigens CD23 and CD19, as well as weak expression of CD20, CD79 and the

surface membrane immunoglobulin, relative to healthy B cells, also need to be confirmed (Fabbri & Dalla-Favera 2016; Hallek et al. 2008).

CLL is a heterogeneous disease where the clinical courses are extremely variable with survivals ranging from one to more than 15 years (Dal-Bo et al. 2009). One third of the patients never need treatment and dies with, not from, the disease, whereas another third initiates an indolent phase, followed by disease progression. The remaining third develops an aggressive disease and needs to start treatment at diagnosis (Dighiero & Hamblin 2008). For patients in the two first groups, CLL is most commonly diagnosed incidentally after a blood test where an asymptomatic increase in number of lymphocytes is detected. Patients with the more aggressive form of CLL will also have swollen lymph nodes, spleen and liver, and bone marrow failure leading to anemia and decreased number of thrombocytes. These clinical findings are the basis for the Rai and Binet staging systems which are widely accepted for setting the prognosis (WHO 2014).

1.1.2 Staging of CLL

The Rai and Binet staging systems (Bazargan et al. 2012; Hallek et al. 2008) are used as the standard basis for assessing prognosis in patients with CLL. They rely on standard laboratory tests and physical examinations that are inexpensive and easy to carry out.

The Rai staging system describes three major prognostic groups divided into subgroups (Table 1). They are based on the prevalence of lymphocytosis (increase in the number of lymphocytes/L above 4×10^9) (Macintyre & Linch 1988) in peripheral blood and bone marrow, swollen lymph nodes, spleen and liver, and reduced number of red blood cells (anemia) and red platelets (thrombocytopenia).

The Binet staging system describes three prognostic stages: stage A, B and C (Table 1). They are based on the prevalence of anemia, thrombocytopenia, and on the number of involved areas with enlarged lymph nodes including head, neck, axillae and groins lymph nodes, as well as enlarged liver and spleen.

Even though these two systems are the standard basis to assess prognosis, they provide no insight into the risk and course of the disease for individual patients and patients diagnosed at an early stage (Binet A or Rai 0 to II disease) (Bazargan et al. 2012). To predict disease progression on an individual basis and for patients in an early stage several biological and cellular markers have proven helpful (Dighiero & Hamblin 2008).

Table 1. Staging systems for CLL.

Rai staging system		Clinical characteristics
0	**Low-risk**	Lymphocytosis in peripheral blood and bone marrow
I	**Intermediate-risk**	Lymphocytosis and enlarged lymph nodes
II		Lymphocytosis and enlarged spleen and/or liver
III	**High-risk**	Lymphocytosis and anemia
IV		Lymphocytosis and thrombocytopenia
Binet staging system		
A		Hemoglobin level ≥10 g/dL, red platelet count ≥100 x 10^9/L and < 3 areas involved
B		Hemoglobin level ≥10 g/dL, red platelet count ≥100 x 10^9/L and ≥ 3 areas involved
C		Hemoglobin level <10 g/dL and/or red platelet count <100 x 10^9/L independent of number of areas involved

1.1.3 Biological markers of CLL and their prognostic impact

Several molecular and cellular markers that can predict disease progression and the choice of treatment have been identified. In particular, immunoglobulin gene mutational status, chromosomal abnormalities and the expression level of CD38 and ZAP70 are well established prognostic markers.

1.1.3.1 Mutational status of the immunoglobulin variable genes

CLL patients can be grouped into two main subgroups defined by the mutational status of the immunoglobulin heavy chain variable region (IgHV). Patients with a mutated phenotype (M-CLL) have the more favorable disease course with longer survival time. It is suggested that the M-CLL is derived from CD27-positive ($CD27^+$) memory B cells, which have undergone somatic hypermutations in the germinal center after T-cell dependent antigen presentation (Figure 1). The unmutated phenotype (UM-CLL) is suggested to derive from $CD27^-$ naïve B cells that are independent of T-cell antigen presentation. In the latter scenario, antigen presentation rather occurs in the marginal zone around the lymphoid follicles, usually in response to carbohydrates or encapsulated viruses or bacteria (Figure 1). The cells will therefore become effector or memory B cells which have not undergone any somatic hypermutations, and thus stay unmutated. The mutational status can be detected by comparing the DNA in B cells with the DNA in the germ line, where a difference of 2% or more defines the mutated subgroup (Chiorazzi et al. 2005; Fabbri & Dalla-Favera 2016).

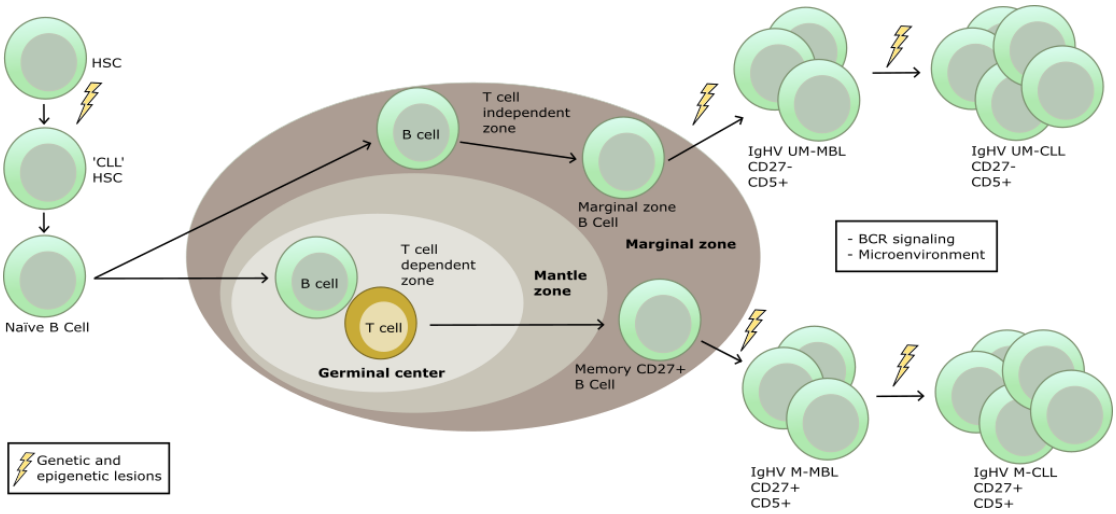

Figure 1. **Origin of M- and UM-CLL.** CLL precursors may originate already at the stem cell stage due to genetic lesions (including *SF3B1* and *NOTCH1*) in the hematopoietic stem cells (HSCs). Naïve precursor CLL B cells will enter the germinal center in the lymph node where they undergo T-cell dependent antigen-presentation, or they will enter the marginal zone where they undergo T-cell independent antigen-presentation. From here, independently of the previous event, they aquire new genetic or epigenetic lesions, proceeding to unmutated monoclonal B cell lymphocytes (UM-MBL) or mutated MBL (M-MBL). Thereafter, the CLL cells aquire another new genetic lesions followed by BCR signaling induced by microenvironmental antigens leading to UM-CLL and M-CLL (Ciccone et al. 2014). Modified from (Ciccone et al. 2014; Fabbri & Dalla-Favera 2016).

1.1.3.2 CD38 and ZAP70

Cluster of differentiation (CD) 38 is a transmembrane glycoprotein which functions both as a receptor and an enzyme with the ability to regulate cell proliferation and survival through signal transmission. According to several studies (Durig et al. 2002; Hock et al. 2010), a high fraction of $CD38^+$ CLL cells can be used as a marker for a more aggressive disease, meaning shorter time to first treatment and shorter overall survival. Evaluation of CD38 expression by flow cytometry is a relatively rapid and low-cost technique which is used as part of the routine diagnostic of CLL patients. Originally, the optimal threshold to classify CD38 positive cells was set to 30%, but this threshold is debated, ranging from 7 – 30% (Van Bockstaele et al. 2009). When evaluating CD38 as a prognostic marker, it is also important to keep in mind that expression of the antigen may vary over time and that some subgroups of patients have bimodal expression of CD38. CD38 expression was in the initial report of Damle et al. (Damle et al. 1999) proposed as a surrogate marker for the IgHV mutational status, but later studies rejected this association, and CD38 should rather be considered as an independent predictor for prognosis in CLL (Van Bockstaele et al. 2009).

The 70 kDa zeta-associated protein (ZAP70) protein is normally expressed by natural

killer and T cells and is one of the membrane components associated with early cell activation, but it has also been reported to be expressed in B cells, including bone marrow and splenic B cells (Van Bockstaele et al. 2009). Its expression in CLL cells has been proposed as a surrogate marker for the IgHV mutational status because of its association with UM-CLL. However, as for CD38, it should rather be considered as a supplement factor in the diagnosis of CLL. Expression of ZAP70 is reportedly associated with a significantly shorter time to progression and overall survival irrespective of the IgHV mutational status (Bazargan et al. 2012). In general, patients characterized as M-CLL, with few CD38 expressing cells and no ZAP70 expression are associated with an indolent course, while the opposite characteristics are associated with an aggressive course.

1.1.3.3 Chromosomal abnormalities

Fluorescence *in situ* hybridization (FISH) has revealed that more than 80% of CLL patients have chromosomal abnormalities which serve as important, independent predictors of disease progression and survival (Bazargan et al. 2012). FISH probe panels are therefore routinely used for chromosomal classifications in CLL. The abnormalities are usually absent early in the course of the disease, but they can appear as the disease progresses. Several chromosomal aberrations are observed in CLL of which 17p13 and 11q22-q23 deletions, 12q13 trisomy and 13q14 deletion are the most frequent (Bazargan et al. 2012; Chiorazzi et al. 2005).

The prognosis is worst for patients with 17p13 deletions, followed by 11q22-q23 deletions, with a frequency in CLL patients of 7 and 16%, respectively. The 17p13 deletion includes the *TP53* gene while the 11q22-23 includes the *ataxia-telangiectasia* gene. Both genes regulate apoptosis and their losses may mediate chemotherapy resistance. For these two groups, the median overall survival time is 32 and 79 months after diagnosis, and the median treatment-free survival time is 9 and 13 months, respectively (Bazargan et al. 2012). Patients with 17p13 or 11q22-q23 deletions are also more symptomatic compared to the other groups, with enlarged lymph nodes and spleen, and also the prevalence of fever, night sweat, weight loss and lower levels of hemoglobin and red platelets are more frequently observed in these two groups. Both the 17p13 and 11q22-23 deletions are also more often associated with UM-CLL (Bazargan et al. 2012; Chiorazzi et al. 2005; Döhner et al. 2000; Fabbri & Dalla-Favera 2016).

The frequency of 12q13 trisomy in CLL patients is reported to be 16%, independent of the mutational status of the immunoglobulin gene (Döhner et al. 2000). Historically, this deletion

was associated with intermediate risk, but more recently, in co-occurrence with mutations in the *NOTCH1* gene, it has been associated with poorer survival (Fabbri & Dalla-Favera 2016). It is suggested that *NOTCH1* mutations lead to increased expression of transcripts involved in pro-survival and anti-apoptotic signals. 12q13p trisomy has also been associated with higher risk of spread to another part of the body and transformation into a more aggressive disease (Richter's syndrome). In general, the median overall survival and the median treatment-free survival time is longer compared to 17p13 and 11q22-q23 deletions, with 114 and 33 months, respectively (Bazargan et al. 2012; Fabbri & Dalla-Favera 2016).

The most frequent aberration is deletion of 13q14 (55% frequency), which appears relatively often in the early stage of CLL and more frequently in M-CLL. This deletion corresponds to the most favorable course of disease if it appears alone, with a median overall survival and median treatment-free survival time reported to be 133 and 92 months, respectively (Döhner et al. 2000; Fabbri & Dalla-Favera 2016).

1.1.4 Treatment

As long as the patient is diagnosed with an early stage and is asymptomatic (Rai 0 and Binet A), treatment is not recommended, unless there is evidence of progression. Standard management for CLL, therefore, includes watchful waiting until the first symptoms of progression are noted or in case of aggressive disease. According to iwCLL, only patients with an active disease require treatment. Generally accepted indicators for an active disease are i) the Rai stage III and IV, or Binet stage C, with progression; ii) enlarged lymph nodes (longest dimension >10 cm), spleen or liver; iii) anemia and thrombocytopenia due to bone marrow failure; iv) progressive lymphocytosis where the lymphocyte doubling time is less than six months or where the number of lymphocytes increase more than 50% within 2 months; v) general symptoms like prolonged fever and night sweat, and unintentional weight loss of over 10% and vi) Richter's syndrome (Hallek et al. 2008; Hus & Rolinski 2015).

Standard treatments for CLL in young patients (age <65 years) with good general condition are combinations of purine analogues, alkylating agents and monoclonal antibodies, including fludarabine, cyclophosphamide and the CD20-specific antibody rituximab (Fabbri & Dalla-Favera 2016; Furman et al. 2014) (Table 2). These regimens usually provide high response rates, but are also associated with toxic effects, and are thus not recommended for elderly patients despite the same health status. Fit, elderly patients should instead be treated with less

toxic regimes, including bendamustine and rituximab. For patients with relapsed CLL or coexisting illness, and for high-risk patients, the guidelines are rituximab alone or in combination with the phosphatidylinositol 3-kinase δ (PI3Kδ) inhibitor idelalisib, or the Bruton's tyrosine kinase (Btk) inhibitor ibrutinib (Furman et al. 2014; Hus & Rolinski 2015). There are also several other drugs in use for treatment of CLL, and Table 2 lists these drugs. The drugs described in the following subsections are drugs investigated in this thesis.

1.1.4.1 Fludarabine

Fludarabine is a purine analogue which is used for effective treatment in indolent leukemia, but also in dividing cells where it can be incorporated into the DNA. It is taken up as fludarabine monophosphate (F-ara-A) through the nucleoside transporter in the cell membrane. Within the cell, it is phosphorylated to fludarabine triphosphate (F-ara-ATP) by a cellular kinase, deoxycytidine kinase (dCK). The activity of dCK is high in lymphocytes, leading to accumulation of F-ara-ATP in these cells. As F-ara-A, fludarabine inhibits DNA polymerase, while F-ara-ATP is incorporated into the DNA, and can also be incorporated into RNA (Fidias et al. 1996). Fludarabine has been reported to be a signal transducer and activator of transcription 1 (STAT1) inhibitor (Frank et al. 1999).

Table 2. Drugs in use for the treatment of CLL. The underlined drugs are studied in this thesis and the italicized drugs may be relevant for treatment.

Alkylating agents:	**Signaling pathway inhibitors:**
Cyclophosphamide, chlorambucil	Btk inhibitor; ibrutinib
bendamustine	PI3K-inhibitor; idelalisib
Anthracyclines:	SYK inhibitor; *fostamatinib*, *P505-15*
Doxorubicin	Protein-kinase inhibitor; *flavopirodol*
Purine analogs:	BCL-2 inhibitor; *oblimersen*, *venetoclax*
Fludarabine, cladribine, pentostatin	**Monoclonal antibodies:**
Vinca alkaloids:	Anti-CD20 antibodies; rituximab, ofatumumab
Vincristine	obinotuzumab
Corticosteroids:	Anti-CD25 antibody; alemtuzumab
Prednisone, methylprednisolone	Anti-CD23 antibody; *lumiliximab*
	Anti-CD38 antibody; *daratumumab*
	Anti-CD40 antibody; *lucatumumab*

1.1.4.2 Vincristine

Vincristine is a naturally occurring molecule extracted from the leaves of the *Catharanthus roseus.* Already in the 17th century, Vincristine was known for its medical use to stop bleeding, to relieve toothaches and to reduce high blood sugar, but it was first in the 1960s that it was

introduced as cancer chemotherapy. The drug was first used as part of combination regimes such as COP and CHOP (C: cyclophosphamide, H: adriamycin, O: vincristine and P: prednisone) in the treatment of other B-cell cancers, before it was introduced for treatment of CLL. The use of vincristine is more frequent in children compared to adults. Children have a greater tolerance to relatively high doses of vincristine, and the tumor in children is more responsive to the drug. The most established effect of vincristine is to bind to, and therefore damage microtubules in the mitotic spindle, resulting in inhibition of mitosis. The spindle structure is damaged in a concentration-dependent manner (Gidding et al. 1999; Vilpo et al. 2000).

1.1.4.3 Doxorubicin

Doxorubicin is one of the most potent chemotherapeutic drugs regarding treatment efficacy. It inhibits topoisomerase I and II, and it can induce programmed cell death by intercalating with the DNA. It has the potential to combat rapidly dividing cells and to slow down disease progression, but it also affects noncancerous cells (Tacar et al. 2013).

1.1.4.4 Idelalisib

Idelalisib, also known as CAL-101, is used both as a single agent and in combination with rituximab for treatment of patients with relapsed CLL or in those who are less able to undergo standard chemotherapy due to coexisting disease. It is a potent inhibitor, selective for the delta isoform of PI3K (PI3Kδ) which is largely restricted to hematopoietic cells. The PI3Kδ transmits signals from, among others, the B cell receptor (BCR), and is important for B-cell homeostasis and function. Inhibition of PI3Kδ promotes apoptosis in B-cell malignancies, including CLL (Do et al. 2016; Hoellenriegel et al. 2011).

1.2 Key signaling pathways in CLL

The human genome comprises more than 20 000 genes of which approximately 1 800 code for proteins involved in intracellular signaling. These proteins control events such as metabolism, differentiation, migration, proliferation, survival and apoptosis, and they are often affected in disease (Rogne & Tasken 2013). The BCR pathway with its associated signaling proteins is essential for normal immune function and for survival and proliferation of B cells. Knowing that the mutational status of the immunoglobulin variable region is a strong predictor for disease outcome in CLL, it is clear that the BCR plays an important role in CLL pathogenesis

(Bertacchini et al. 2015). The BCR is composed of covalently linked immunoglobulin heavy and light chains and is tightly associated with the membrane integrated CD79a and b. After antigen stimulation, the BCR propagates an activation signal to a Sacroma (Src)-family protein tyrosine kinase, normally Lyn, which then induces phosphorylation of the immunoreceptor tyrosine-based activation motifs (ITAMs) on CD79a and b (Figure 2). Phosphorylated ITAMs serve as docking sites for SH2-domain containing proteins, most often Spleen tyrosine kinase (SYK). SYK can be replaced by ZAP70 which is, as mentioned, expressed in CLL cells with an aggressive course. The signaling continues with formation of the BCR signalosome which starts with the recruitment of B cell linker protein (BLNK) to CD79b. BLNK serves as a docking site for Btk, Phospholipase Cγ2 (PLCγ2) and the adaptor protein Growth factor receptor-bound protein 2 (GRB2), among others. This BCR signalosome generates a wide variety of downstream effects, including activation of the PI3K-Akt-mTOR pathway and the Ras-Raf-MEK-ERK pathway (Zhong et al. 2014).

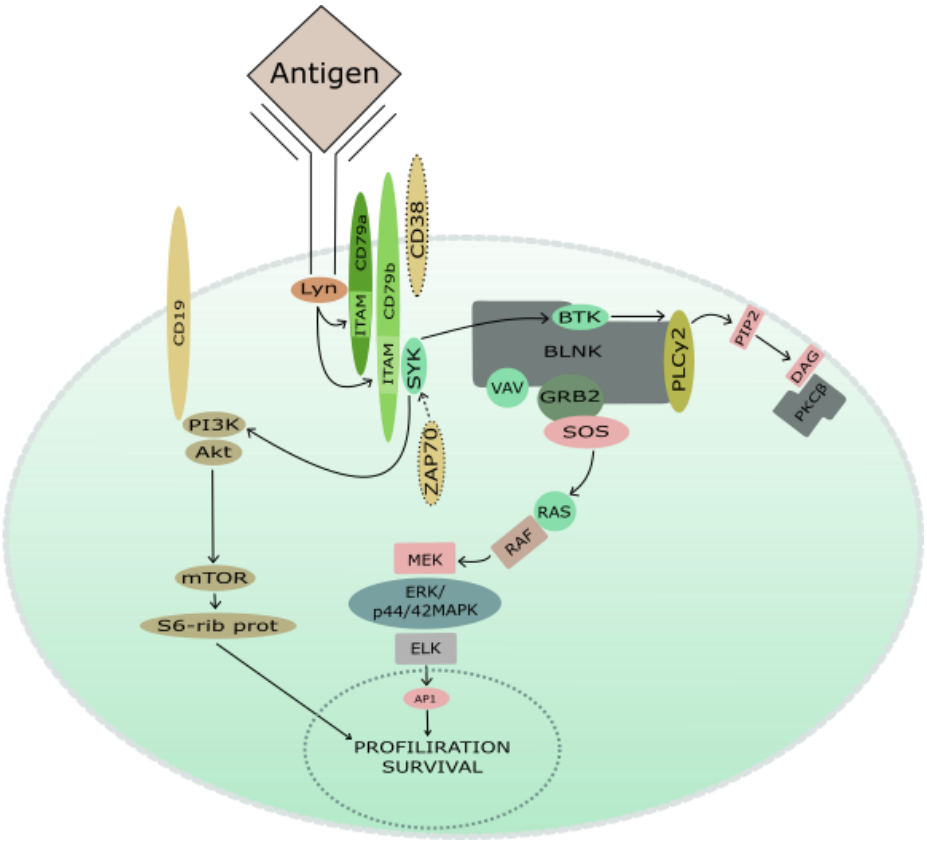

Figure 2. B-cell receptor signaling. Ligation of the BCR induces a signaling cascade through CD79a and b and signalosome including BLNK, PLCγ2, GRB2, VAV and Btk before signals diverge in different pathways. Presence of ZAP70 and CD38 indicate disease progression in CLL. Modified from (Ciccone et al. 2014; Zhong et al. 2014).

After assembly of the BCR signalosome, a signaling through GRB2, the Son of sevenless (SOS) and rat sarcoma protein (Ras) is propagated downstream leading to activation of the Raf proto-oncogene serine/threonine-protein kinase (Raf) followed by Mitogen activated protein kinase kinase (MEK) and Mitogen activated protein kinase (p44/42 MAPK/ERK). This Ras-Raf-MEK-ERK pathway regulates the expression of the Activator protein 1 (AP1) which is a transcription factor important for proliferation and differentiation (Zhong et al. 2014).

The PI3K-Akt-mTOR pathway is involved in many cellular functions, including cell cycle progression, cell survival and apoptosis. It is one of the most commonly mutated pathways in cancer and increased activity of the pathway has been observed in many malignancies, including leukemia (Bertacchini et al. 2015). After BCR activation, the PI3K converts phosphatidylinositol-4,5-bisphosphate (PIP_2) to phosphatidylinositol-3,4,5-trisphosphate (PIP_3), which serves as a docking site for Akt and Phosphoinositide-dependent protein kinase 1 (PDK1). Mammalian target of rapamycin (mTOR) is recruited, and both mTOR and PDK1 phosphorylate Akt. Fully activated Akt phosphorylates various target proteins, leading to inhibition of apoptosis and promotion of cell survival (Bertacchini et al. 2015).

A central signaling pathway in CLL is the JAK/STAT pathway (Burgler et al. 2015). Activation of this pathway stimulates cell migration, proliferation, differentiation and apoptosis which are crucial for growth and development of the immune system (Rawlings et al. 2004). When a ligand, such as a growth hormone or an interferon, such as Interferon γ (IFNγ), binds to its cognate receptor, a receptor dimer is formed and Janus kinase (JAK) tyrosine kinases are recruited. The JAKs phosphorylate additional targets, including the STATs. The STATs are latent transcription factors ready to activate or repress transcription of target genes, including CD38 (Burgler et al. 2015; Rawlings et al. 2004).

1.3 Phosphoflow cytometry

Phosphoflow cytometry is a phospho-specific flow cytometry-based approach which makes it possible to measure the phosphorylation status of signaling proteins at a single-cell level. The technique can be combined with fluorescent cell barcoding (FCB) which makes it possible to analyse multiple samples at the same time (Krutzik & Nolan 2006). To this end, cells are stained with unique combinations and dilutions of one or more florescent dyes before they are combined in one experimental tube (Krutzik & Nolan 2006; Landskron & Tasken 2016; Rogne & Tasken

2013) (Figure 3). Changes in the phosphorylation status reflect changes in protein activity. Aberrations in the signaling pattern can indicate drug targets and expand our knowledge regarding phosphorylation cascades (Rogne & Tasken 2013).

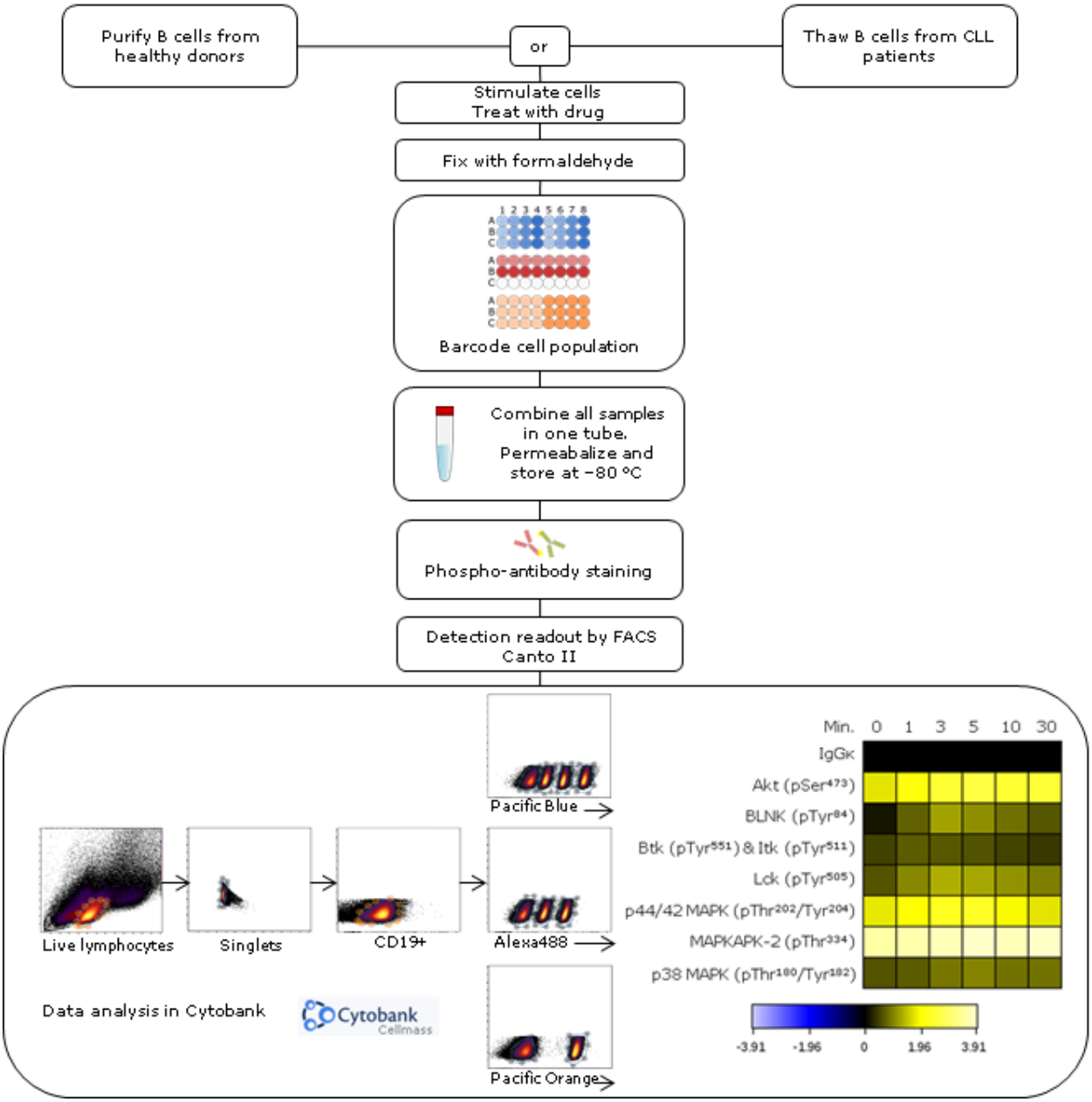

Figure 3. Work flow for phosphoflow cytometry. B cells from healthy donors or CLL patients were incubated with DMSO (0,001%) or one of three cytostatic drugs for 20 minutes followed by stimulation with anti-IgM or sCD40L. The cells were then fixed, barcoded and permeabilized before they were distributed into aliquots. Each aliquot was stained with anti-CD19 surface marker and one of 20 different phospho-antibodies or IgGκ as a control. The fluorescence signals were detected by flow cytometry and the data were analysed in Cytobank.

2 Objectives

CLL is a heterogeneous disease with variable clinical courses. Although the disease is incurable, a third to half of the patients may never need treatment. For those who need treatment, the options are limited and it is important to prevent them from exposure to ineffective therapy. Furthermore, the prevalence of CLL is growing steeply which raises the need for treatment options beyond second line. The work presented in this master thesis is part of a larger project in the group of Professor Dr. med. Kjetil Taskén co-supervised by researcher Dr. Sigrid S. Skånland, and in collaboration with Oslo University Hospital, Rikshospitalet. The ultimate goal of the project is to tailor the treatment of CLL patients on an individual basis according to patients' biology and prognosis. The aims of the project as a whole are to:

1: Provide patient benefit to the same patient who donates a sample.

2: Assist clinical decisions for treatment beyond second line.

3: Identify drug combinations which will be efficient for the individual patient.

The more specific main goals of the work presented here have been to:

1: Establish phosphoflow cytometry as a method to analyse protein phosphorylation in B cells from CLL patients and healthy donors in the lab. This is a relatively fast approach which should make it possible, in the future, to give benefit to the same patient who donates a sample.

2: Analyse basal and induced signaling in CLL cells relative to healthy controls in order to map signaling aberrations which can provide indications for targeted therapy.

3: Investigate the effect of the cytostatic drugs fludarabine, doxorubicin and vincristine on basal and induced B cell signaling. These drugs are currently in use for the treatment of CLL and will be used in combination studies in future large-scale drug screens. Observed effects on signaling may indicate combinatorial drug candidates which may benefit the patient.

3 Materials and Methods

3.1 Patient material and ethical considerations

Buffy coats from healthy blood donors and frozen CLL cells from patients were received from the Blood Centre (Oslo University Hospital) and the Department of Haematology, Oslo University Hospital, Rikshospitalet, respectively, with consent from all the donors. The study is approved by the Regional Ethical Committee and the research on human blood was carried out in accordance with the Declaration of Helsinki (2013).

3.2 Reagents and antibodies

The cytostatic drugs fludarabine (Cat. # S1491), doxorubicin (adriamycin) (Cat. # S1208) and vincristine (Cat. # S1241), and the inhibitor idelalisib (Cat. # S2226) were from Selleckchem (Houston, TX, USA). Alexa Fluor 647-conjugated antibodies against BLNK ($pTyr^{84}$) (Cat. # 558443), Btk ($pTyr^{551}$) & Itk ($pTyr^{511}$) (Cat. # 558129), IgGkappa (Cat. # 557783), Lck ($pTyr^{505}$) (Cat. # 558577), MEK1 ($pSer^{298}$) (Cat. # 560043), NF-κB p65 ($pSer^{529}$) (Cat. # 558422), PLCγ2 ($pTyr^{759}$) (Cat. # 558498), Rb (pSer807/811) (Cat. # 558590), STAT1 ($pTyr^{701}$) (Cat. # 612597), STAT3 ($pTyr^{705}$) (Cat. # 557815), STAT5 ($pTyr^{694}$) (Cat. # 612599) and STAT6 ($pTyr^{641}$) (Cat. # 612601) were from BD Biosciences (Franklin Lakes, NJ, USA). Alexa Fluor 647-conjugated Akt ($pSer^{473}$) (Cat. # 4075), Histone H3 ($pSer^{10}$) (Cat. # 9716), MAPKAPK-2 ($pThr^{334}$) (Cat. # 4320), p44/42 MAPK ($pThr^{202}$/Tyr^{204}) (Cat. # 4375), NF-κB p65 ($pSer^{536}$) (Cat. # 4887), p38 MAPK ($pThr^{180}$/Tyr^{182}) (Cat. # 4552), SAPK/JNK ($pThr^{183}$/Tyr^{185}) (Cat. # 9257), S6-Ribosomal protein kinase ($pSer^{235/236}$) (Cat. # 4851), and SYK ($pTyr^{525/526}$) (Cat. # 12081) were from Cell Signaling (Danvers, MA, USA). The anti-human surface markers PerCP-Cy5.5-conjugated CD5 (Cat. # 45-0058) and CD19 (Cat. # 45-0199) were from eBioscience (San Diego, CA, USA). APC-conjugated CD19 (Cat. # 21270196) and PE-conjugated CD38 (Cat. # 21270384) were from ImmunoTools (Friesoythe, Germany) and FITC-conjugated CD40 (Cat. # 334306) was from BioLegend (San Diego, CA, USA). The anti-human IgM (Cat. # 2022-01) was from Southern Biotechnology (Birmingham, AL, USA), and sCD40L (Cat. # 11343345) and IFNγ (Cat. # 11343534) were from ImmunoTools. The RosetteSep™ Human B Cell Enrichment Cocktails (Cat. # 15064) and Lymphoprep™ (Cat. # 07861) were from Stemcell Technologies (Cambridge, United Kingdom). The BD phosphoflow™ Perm Buffer III (Cat. # 558050) and Fix

Buffer I (Cat. # 557870) were from BD Bioscience. The RPMI 1640 GlutaMAX™ medium (Cat. # 61870044), fetal calf serum (FCS) (Cat. # 10270106) and the barcoding fluorochromes Ax488 Succinimidyl Ester (Cat. # A20100), Pacific Blue Succinimidyl Ester (Cat. # P10163) and Pacific Orange Succinimidyl Ester (Cat. # P30253) were from Thermo Fisher Scientific (Waltham, MA, USA). The Trypsin-EDTA (Cat. # BE17-161E) was from Lonza (Basel, Zwitzerland). Bovine serum albumin (BSA) was from Sigma (St. Louis, MO, USA).

3.3 Phosphoflow experiments

The phosphoflow experiments were performed as described previously (Skånland et al. 2014), but with some modifications, and on B cells from healthy donors or CLL patients instead of T cells. See the following subsections.

3.3.1 Purification of B lymphocytes from buffy coat

B cells were purified from buffy coats by negative selection using RosetteSep^{TM} Human B Cell Enrichment Cocktails (20 µl/ml blood). After 20 minutes incubation, Lymphoprep^{TM}, a density gradient medium, was added to the blood diluted (1:1) in PBS with 2% FCS, and it was centrifuged for 25 min at 800g at 4°C. After centrifugation the cells were harvested and washed in PBS with 2% FCS and centrifuged for 15 min at 250g. Purification was performed according to the manufacturers' protocol for both RosetteSep^{TM} and Lymphoprep^{TM}.

3.3.2 Stimulation and fixation

Freshly purified B cells from healthy donors or B cells thawed and incubated at 37°C over-night from CLL patients, were resuspended in RPMI 1640 GlutaMAX™ medium with 1 or 10% FCS for the short and long time-course experiments, respectively, and 1% penicillin/streptomycin ($30x10^6$- $60x10^6$ cells/ml). The cells were incubated for 10 minutes in a 37°C water bath or incubator, before pre-incubation as indicated with drugs or 0,001% DMSO as control, for 20 min. An unstimulated sample was taken out before the cells were stimulated with anti-IgM (1 µg/ml) or sCD40L (400 ng/ml), and the cells were left in the water bath or in the incubator for a short (1-3-5-10-30 min) or long (3-16-24 h) time span, respectively. The harvested samples were fixed for 10 minutes in pre-warmed BD Phosphoflow™ Fix Buffer I at 37°C followed by two washes with PBS. Four unstimulated samples were separated and fixed for use as compensation controls.

3.3.3 FCB

Fixed cells were resuspended in PBS and incubated with different concentrations of the barcoding fluorochromes Alexa Fluor® 488, Pacific Orange and Pacific Blue (diluted in DMSO) in a 96-v-well plate. After staining in the dark for 20 min at room temperature, the cells were washed twice with flow wash (PBS, 10% FCS and 0,08% sodium azide), combined in one tube and permeabilized with BD Phosphoflow™ Perm Buffer III pre-stored at -20°C, and stored at -80°C.

3.3.4 Antibody staining and phosphoflow cytometry analysis

The permeabilized cells were washed three times with flow wash and spun for 5 min at 500g, resuspended and distributed into aliquots. The aliquots were stained with anti-CD19 surface marker conjugated with PerCP-Cy5.5 and the indicated phospho-specific antibodies, conjugated with Alexa Fluor® 647, before they were incubated in the dark at room temperature for 30 min. Next, the samples were washed once, resuspended with flow wash and analysed with a BD FACSCanto II (4-2-2) cytometer equipped with 405 nm, 488 nm and 633 nm lasers. Separately, unstimulated cells stained with Alexa Fluor® 488, Pacific Orange and Pacific Blue, and compensation beads incubated with PerCP-Cy5.5 and Alexa Fluor® 647, were used for compensation. 150 000-500 000 events were recorded per sample. Signals were calculated using the inverse hyperbolic sine (arcsinh) of the MFI (median fluorescent intensity) of stimulated versus unstimulated cell populations, as explained by Irish et al. (Irish et al. 2010).

3.3.5 Analysis in Cytobank

The data were analysed in Cytobank (https://cellmass.cytobank.org/cytobank/). By plotting SSC area versus FSC area, the live lymphocytes were selected. Thereafter, single cells were selected by plotting FSC height versus FSC width. $CD19^+$ cells were selected by plotting SSC area versus PerCP-Cy5.5 and the FCB was selected by plotting Alexa Fluor® 488, Pacific Blue and Pacific Orange against SSC area sequentially.

3.4 Stimulation and surface staining of B cells from CLL patients

CD40L transfected or untransfected fibroblasts (NIH-3T3) were detached from the cell culture flask with trypsin-EDTA for 5 min at 37°C. RPMI with 10% FCS was added, and the detached fibroblasts were harvested, followed by three washes with RPMI 10% FCS. The CD40L-

transfected and untransfected fibroblasts were then irradiated with 50Gy and 125Gy, respectively. CLL cells ($1x10^6$ cells/ml) were co-cultured with fibroblasts ($4x10^5$ cells/ml) and where indicated, with IFNγ (50 ng/ml), fludarabine (1 µM) or DMSO (control) were added to the CLL cells. After two days of stimulation, the CLL cells were harvested and centrifuged for 7 min at 300g. The cells were washed with staining buffer (PBS + 0,5 % BSA) before incubation with APC-conjugated antibodies against human CD19, Per-CP-Cy5,5-conjugated anti-CD5, PE-conjugated anti-CD38 and FITC-conjugated anti-CD40 for 30 minutes on ice. The stained cells were then washed with staining buffer and fixed on ice for 15-20 minutes with staining buffer and paraformaldehyde (1:1), spun down and resuspended with staining buffer and stored at 4°C. The samples were run on a BD FACSCalibur cytometer and the data analysed by FlowJo (Ashland, OR, USA). The live lymphocytes and activated cells (lymphoblasts) were selected by plotting SSC area versus FSC area. Thereafter, single cells were selected by plotting FSC height against FSC width. $CD19^+$ and $CD5^+$ cells were selected by plotting PerCP-Cy5-5 versus APC, and the $CD40^+$ cells were selected by plotting FITC against FSC area.

4 Results

The CLL cells included in the following experiments were from six different patients. For information concerning the investigated patients, see table 3.

Table 3. Patient information.

Patient identifier	Gender/age (years)	Time from diagnosis to procurement (months)	Treatment prior to procurement	Binet stage	IgHV-gene mutational status (% homology germline)	Chromosomal aberrations
CLL125[A,D,+]	M/44		FCA	A at diagnosis, progressed to C	M (97,3%)	Normal karyotype
CLL135[A,B,C,D,+]	M/61		*FCR-A-BR	A at diagnosis, progressed to C	UM (100%)	Normal karyotype
CLL139[A,B]	F/61	82	No	C	M (93,2%)	ND
CLL142	F48	144	No	B	M (96%)	del(13q14), del(17q13, *TP53*mutation)
CLL149	M/50	28	No	A	UM (100%)	ND
CLL150[A,B,C,D]	F/59	76	FCR	B	UM (100%)	del(13q14), del(17q13, *TP53*mutation)

[A] Used in Figure 4A, [B] used in Figure 4B, [C] used in Figure 4C, [D] used in Figure 4D. No; Non-treated patients, ND; not defined. Treated patients have received following drugs marked with aberrations: F=fludarabine; C=cyclophosphamide; A=alemtuzumab; R=rituximab; BR= bendamustine. *CLL135 was initially treated with FCR, then A and finally BR. [+] CD38 expression (%) in CLL125=0, CLL135=50, not defined for the remaining CLL patients.

4.1 Impaired basal levels of phosphorylation in CLL cell samples relative to healthy controls

In order to map signaling aberrations in CLL cells relative to healthy B cells, both basal and induced signaling were investigated. First, basal signaling, with or without the presence of cytostatic drug, were considered. Cytostatic drugs were included to investigate their effects on B-cell signaling. Phosphorylation of 20 different epitopes on signaling proteins relevant for the BCR pathway was used as the readout, and IgGkappa was used as an isotype control.

As shown in Figure 4A, the basal level of phosphorylation in CLL cells was significantly lower for BLNK ($pTyr^{84}$), Btk ($pTyr^{551}$) & Itk ($pTyr^{511}$), Histone H3 ($pSer^{10}$), p38 MAPK ($pThr^{180}/Tyr^{182}$) and S6-Ribosomal protein kinase ($pSer^{235/236}$), while similar for Akt ($pSer^{473}$), Lck ($pTyr^{505}$), p44/42 MAPK ($pThr^{202}/Tyr^{204}$), MAPKAPK-2 ($pThr^{334}$), MEK1 ($pSer^{298}$), NF-κB

p65 (pSer^{529}), NF-κB p65 (pSer^{536}), PLCγ2 (pTyr^{759}), Rb (pSer807/811), SAPK/JNK (pThr^{183}/Tyr^{185}), STAT1 (pTyr^{701}), STAT5 (pTyr^{694}), STAT6 (pTyr^{641}) and SYK (pTyr$^{525/526}$) relative to healthy B cells. For STAT3 (pTyr^{705}) the level of phosphorylation was significantly higher in CLL cells (Figure 4A).

The first cytostatic drug examined to assess the effect on the basal signaling was fludarabine. The working concentrations of the drugs were selected based on a titration curve, as explained below (Figure 6). As for untreated cells, the basal level of phosphorylation was significantly reduced for BLNK (pTyr^{84}), Btk (pTyr^{551}) & Itk (pTyr^{511}), p38 MAPK (pThr^{180}/Tyr^{182}) and S6-Ribosomal protein kinase (pSer$^{235/236}$) in CLL cells compared to healthy B cells. In fludarabine treated cells, the level of phosphorylation was also observed to be significantly lower for PLCγ2 (pTyr^{759}) and SYK (pTyr$^{525/526}$) in CLL cells. For the remaining parameters, the signaling was not significantly different (Figure 4B).

Next, the effect of doxorubicin on basal cell signaling was examined. Due to limited data (n=2), statistical significance could not be calculated. However, the findings suggested a tendency towards reduced phosphorylation of BLNK (pTyr^{84}), Btk (pTyr^{551}) & Itk (pTyr^{511}), Histone H3 (pSer^{10}), p44/42 MAPK (pThr^{202}/Tyr^{204}), MAPKAPK-2 (pThr^{334}), p38 MAPK (pThr^{180}/Tyr^{182}), MEK1 (pSer^{298}), PLCγ2 (pTyr^{759}), S6-Ribosomal protein kinase (pSer$^{235/236}$), SAPK/JNK (pThr^{183}/Tyr^{185}), and SYK (pTyr$^{525/526}$) in CLL patients samples compared to healthy controls in the presence of doxorubicin. As for untreated cells, STAT3 (pTyr^{705}) signaling was higher in CLL cells compared to healthy B cells (Figure 4C).

The last cytostatic drug examined was vincristine, which significantly suppressed the phosphorylation of p44/42 MAPK (pThr^{202}/Tyr^{204}) in CLL cells relative to healthy controls. The differences in the remaining parameters were not significant (Figure 4 D).

Finally, untreated CLL cells were compared to fludarabine, doxorubicin and vincristine treated CLL cells. The basal level of phosphorylation was significantly increased in SAPK/JNK (pThr^{183}/Tyr^{185}) in CLL patients after vincristine treatment (Figure 4E). For the remaining parameters, it was not observed any remarkably differences between treated and untreated patients.

Overall, the basal level of phosphorylation was lower or similar in CLL cells relative to healthy B cells irrespective of drug treatment except for STAT3 (pTyr^{705}), where the signaling was elevated for both untreated and doxorubicin treated CLL cells compared to healthy B cells.

The presence of the cytostatic drugs had some effect on cell signaling. While doxorubicin appeared to induce reduced signaling of additional proteins, vincristine rather leveled out the differences between healthy and CLL cells.

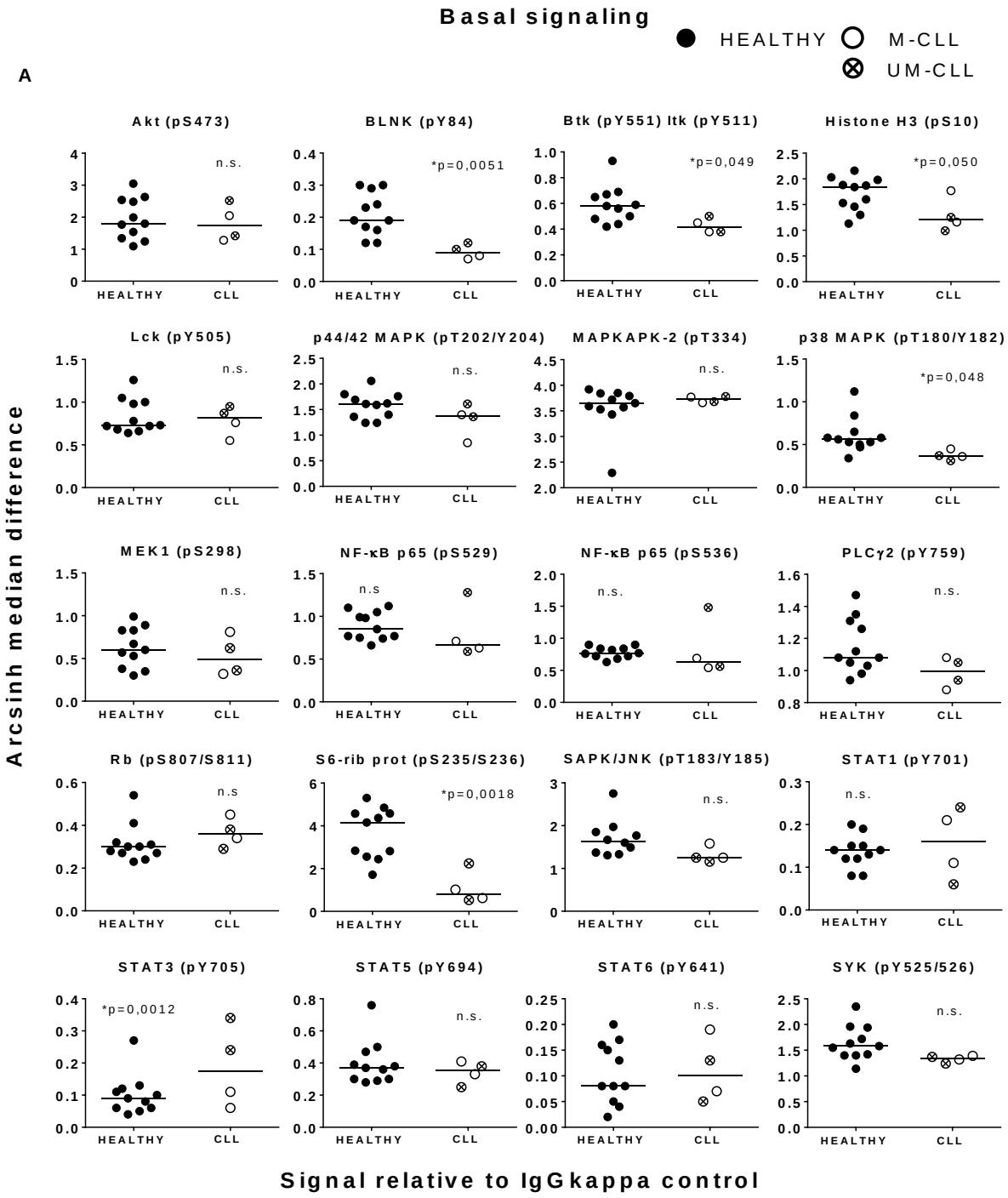

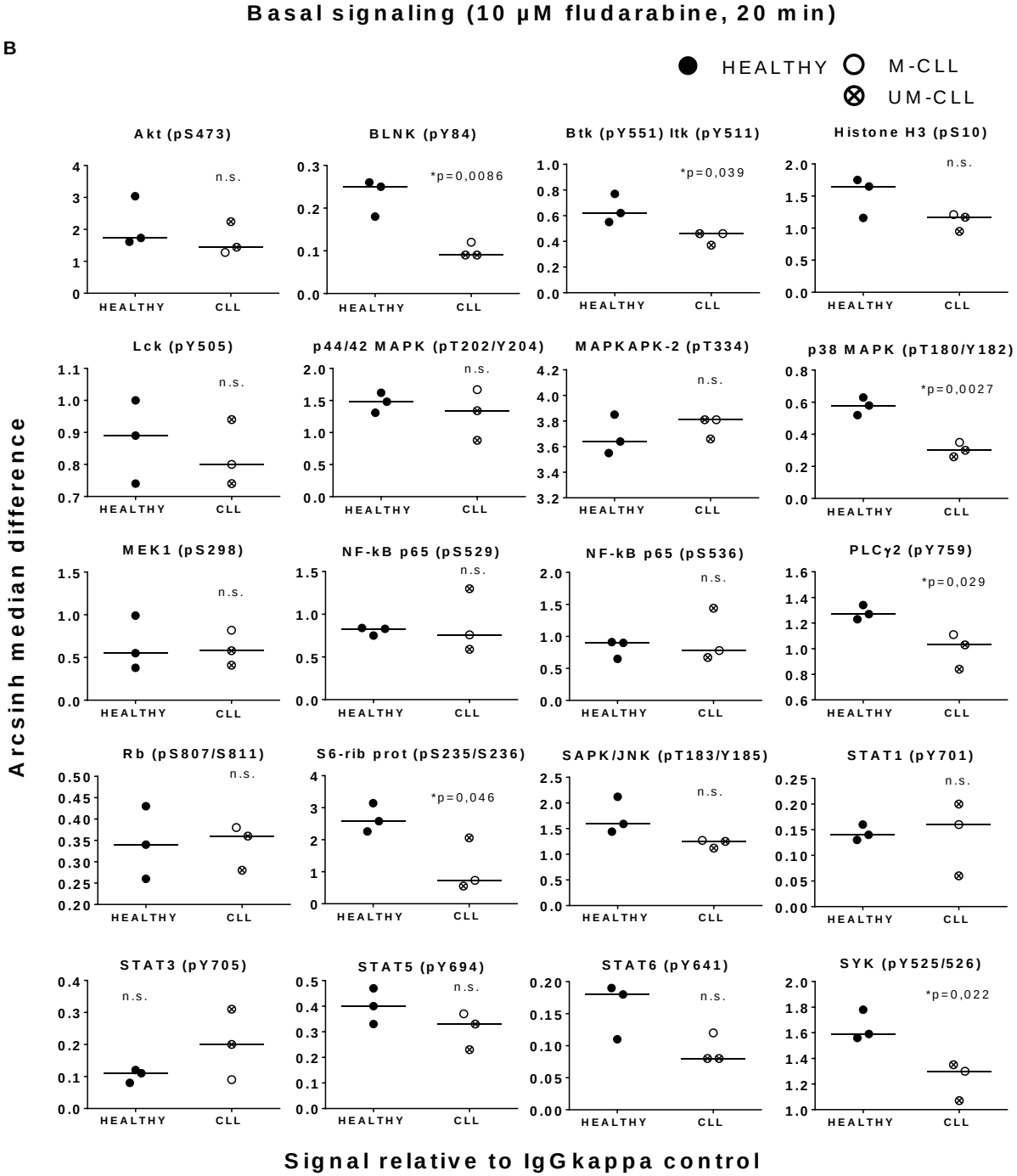
Basal signaling (10 µM fludarabine, 20 min)
B
HEALTHY
M-CLL
UM-CLL
Akt (pS473)
n.s.
BLNK (pY84)
*p=0,0086
Btk (pY551) Itk (pY511)
*p=0,039
Histone H3 (pS10)
n.s.
Lck (pY505)
n.s.
p44/42 MAPK (pT202/Y204)
n.s.
MAPKAPK-2 (pT334)
n.s.
p38 MAPK (pT180/Y182)
*p=0,0027
MEK1 (pS298)
n.s.
NF-kB p65 (pS529)
n.s.
NF-kB p65 (pS536)
n.s.
PLCγ2 (pY759)
*p=0,029
Rb (pS807/S811)
n.s.
S6-rib prot (pS235/S236)
*p=0,046
SAPK/JNK (pT183/Y185)
n.s.
STAT1 (pY701)
n.s.
STAT3 (pY705)
n.s.
STAT5 (pY694)
n.s.
STAT6 (pY641)
n.s.
SYK (pY525/526)
*p=0,022
HEALTHY
CLL
Arcsinh median difference
Signal relative to IgGkappa control

C

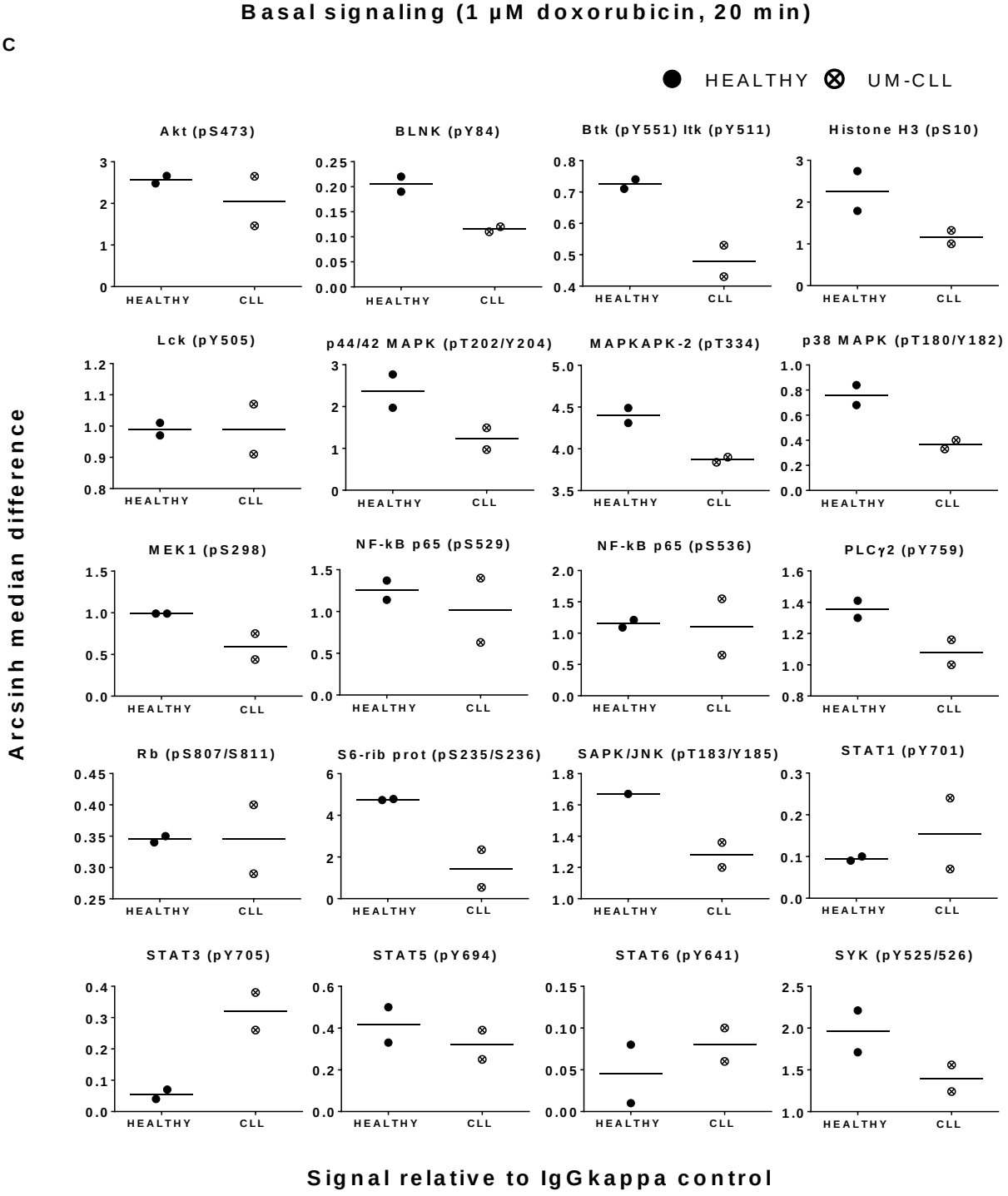
Basal signaling (1 µM doxorubicin, 20 min)
HEALTHY
UM-CLL
Arcsinh median difference
Akt (pS473)
BLNK (pY84)
Btk (pY551) Itk (pY511)
Histone H3 (pS10)
Lck (pY505)
p44/42 MAPK (pT202/Y204)
MAPKAPK-2 (pT334)
p38 MAPK (pT180/Y182)
MEK1 (pS298)
NF-kB p65 (pS529)
NF-kB p65 (pS536)
PLCγ2 (pY759)
Rb (pS807/S811)
S6-rib prot (pS235/S236)
SAPK/JNK (pT183/Y185)
STAT1 (pY701)
STAT3 (pY705)
STAT5 (pY694)
STAT6 (pY641)
SYK (pY525/526)
HEALTHY
CLL
Signal relative to IgGkappa control

Basal signaling (10 µM vincristine, 20 min)

D

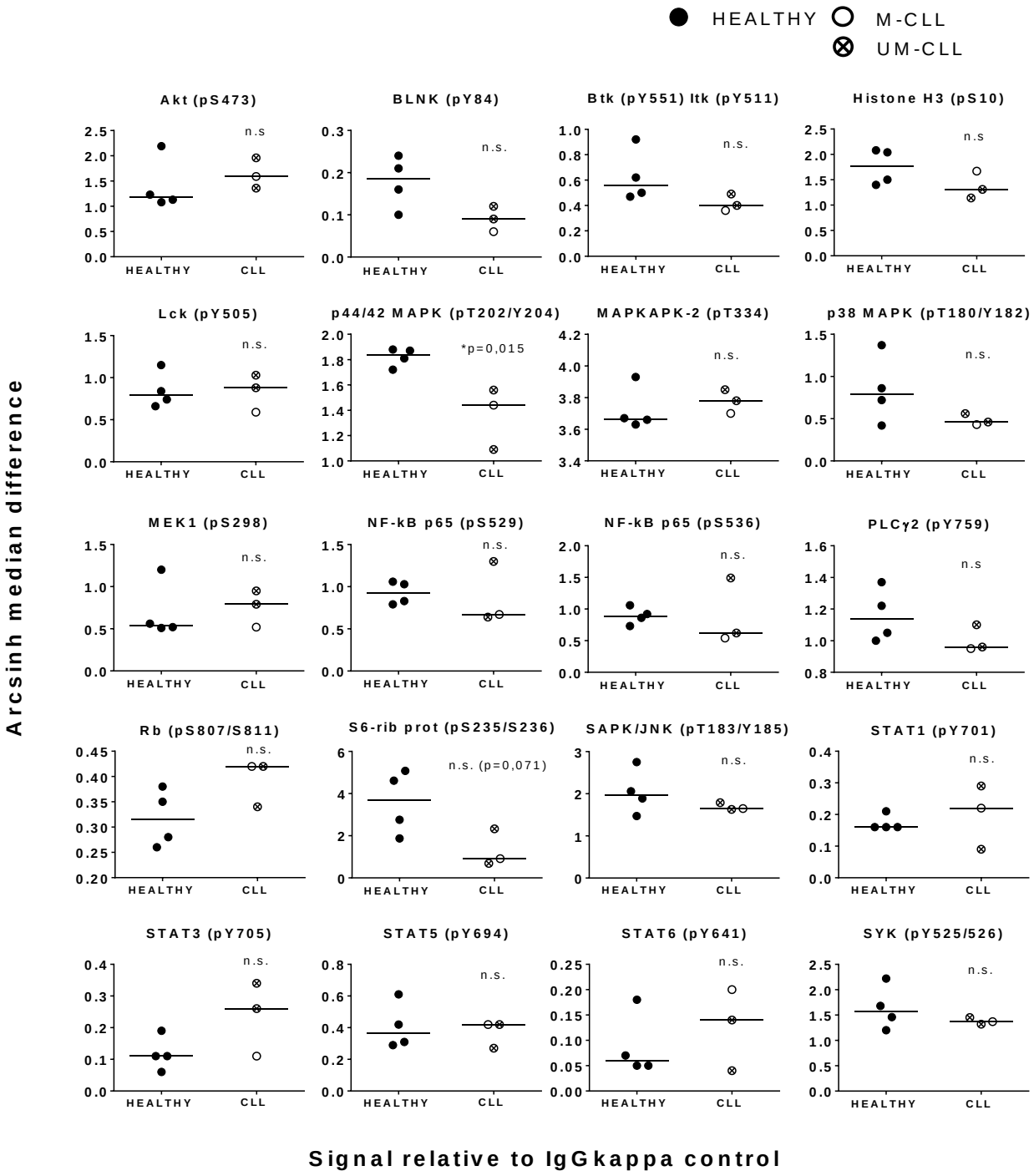

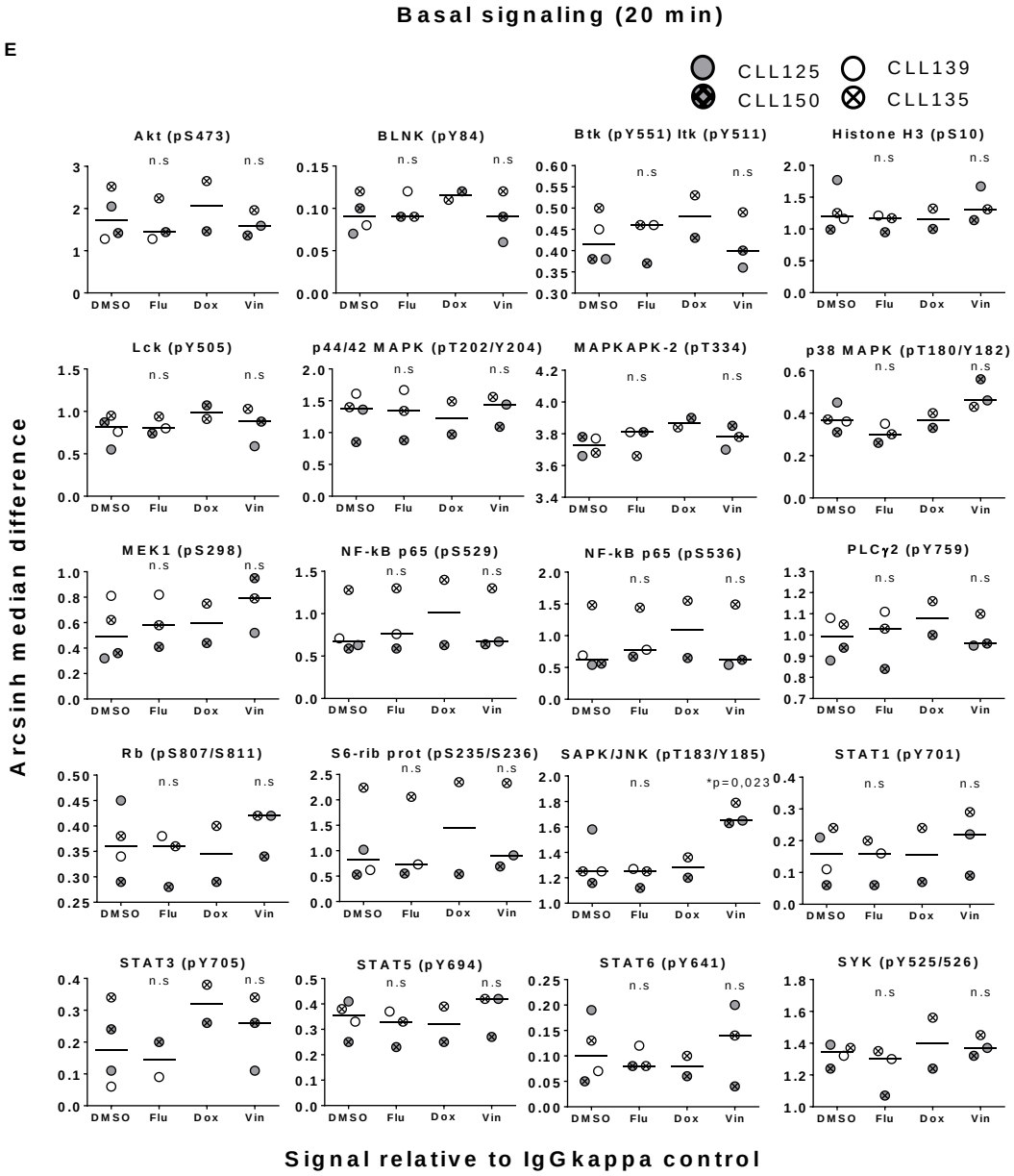

Figure 4. Basal levels of phosphorylation in B cells from healthy donors and CLL patients. A) B cells from healthy donors (n=11) and CLL patients (n=4) were incubated with DMSO (0,001%) for 20 min. The cells were then fixed, barcoded and permeabilized before they were distributed into aliquots. Each aliquot was stained with anti-CD19 surface marker and one of 20 different phospho-antibodies or IgGκ as a control. The fluorescence signals were detected by flow cytometry and the data were analysed in Cytobank. The basal fluorescence intensity signals were measured relative to IgGκ control and shown as arcsinh median difference. * indicates the significant p-value, $p < 0,05$, n.s.: not significant; Student's t-Test. M-CLL; IgHV mutated CLL, UM-CLL; IgHV unmutated CLL. **B)** The experiment was performed as in A), but the cells (healthy n=3, CLL n=3) were incubated with fludarabine (10 μM) instead of DMSO. **C)** The experiment was performed as in A), but the cells (healthy n=2 [except for SAPK/JNK], CLL n=2) were incubated with doxorubicin (1 μM) instead of DMSO. **D)** The experiment was performed as in A), but the cells (healthy n=4, CLL n=3) were incubated with vincristine (10 μM) instead of DMSO. **E)** The presented data are collected from the experiments above. The p-values is calculated relative to the control.

4.2 Elevated signaling in UM-CLL cells in response to anti-IgM stimulation

Next, to map the induced signaling differences in CLL cells relative to healthy controls, the cells were stimulated with anti-IgM for short (1-30 min) (Figure 5) and long (3-24 h) (Supplementary Figure 1) time courses. It has previously been reported that UM-CLL has an increased sensitivity towards anti-IgM stimulation (Fabbri & Dalla-Favera 2016).

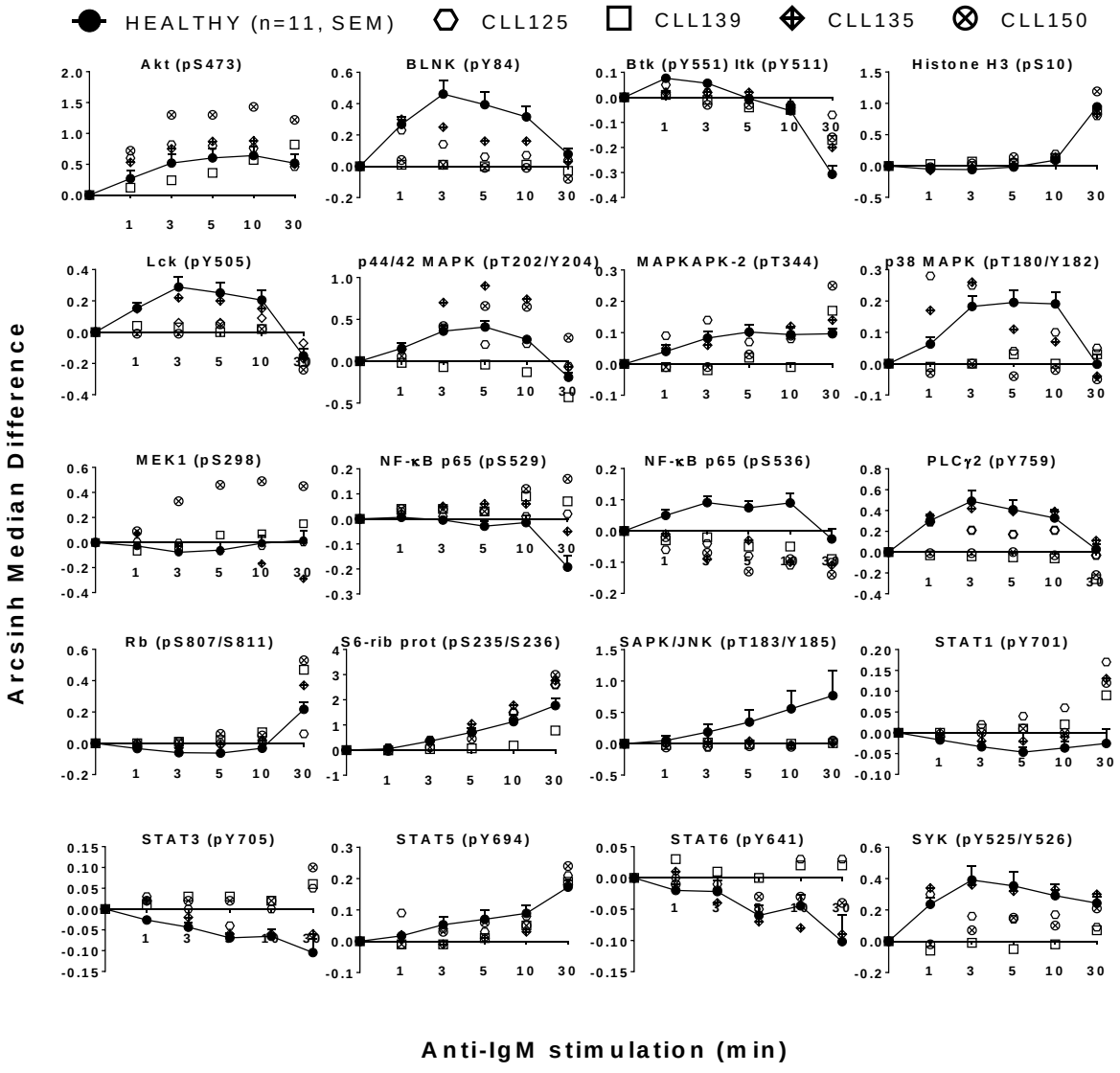

Figure 5. Anti-IgM induced signaling in B cells from healthy donors and CLL patients. B cells from healthy donors (mean + SEM, n=11) and M-CLL125, UM-CLL135, M-CLL139 and UM-CLL150 were stimulated with anti-IgM (1 µg/ml) for the indicated time period, and then processed and analysed as described in Figure 4. The fluorescence intensity signal was measured relative to unstimulated samples and shown as arcsinh median difference.

When cells were stimulated with anti-IgM for up to 30 min, the phosphorylation of Akt (pSer^{473}), p44/42 MAPK (pThr^{202}/Tyr^{204}), and MEK1 (pSer^{298}) was induced in UM-CLL150 cells relative to the average of healthy B cells (Figure 5). The phosphorylation of Akt (pSer^{473}) and p44/42 MAPK (pThr^{202}/Tyr^{204}) was also increased in UM-CLL135. For M-CLL139, the phosphorylation of Akt (pSer^{473}) was reduced. However, for most of the parameters, the CLL cells were hyporesponsive or showed only minor deviations from healthy controls (Figure 5). The increased phosphorylation level of Akt (pSer^{473}), p44/42 MAPK (pThr^{202}/Tyr^{204}) and MEK1 (pSer^{298}) was lost after long stimulation and the overall signal amplitude was much lower as well (3-24 h, see Supplementary Figure 1). Altogether, short stimulation of the BCR pathway induced elevated levels of phosphorylation of Akt (pSer^{473}), p44/42 MAPK (pThr^{202}/Tyr^{204}), and MEK1 (pSer^{298}) in UM-CLL cells.

4.3 Fludarabine and doxorubicin enhance anti-IgM induced signaling

The effect of the cytostatic drugs fludarabine, doxorubicin and vincristine on induced B cell signaling was then studied. In order to determine the optimal working concentrations of these drugs, healthy B cells were treated with three different concentrations (0,1 µM, 1 µM and 10 µM) of the drugs, followed by anti-IgM stimulation (Figure 6).

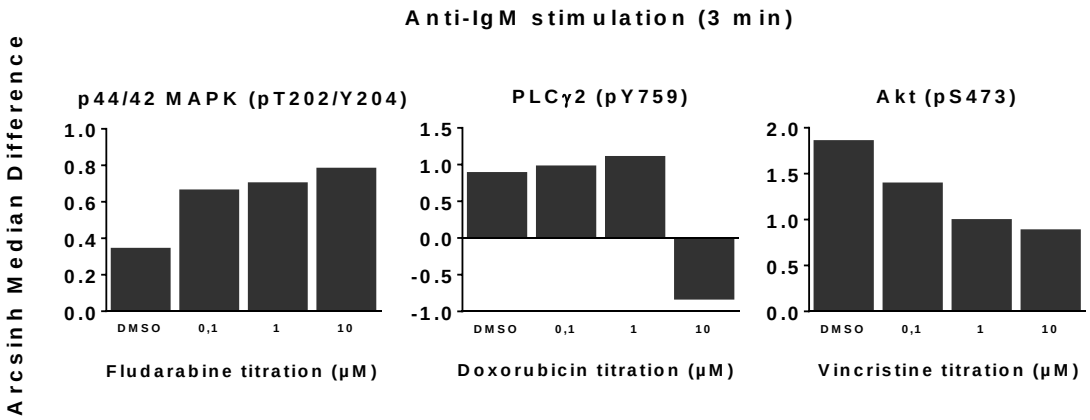

Figure 6. Titration of fludarabine, doxorubicin and vincristine. B cells from healthy donors were incubated with the indicated concentrations of fludarabine, doxorubicin or vincristine for 20 min, before stimulation with anti-IgM (1 µg/ml) for 3 min. The cells were then processed and analysed as described in Figure 5.

The cells responded in a dose-dependent manner to the drugs with the most pronounced effect at the highest concentration. An exception was observed for doxorubicin, which appeared

to be toxic to the cells at 10 µM (Figure 6). Based on these results the working concentrations 10 µM, 1 µM and 10 µM were chosen for fludarabine, doxorubicin and vincristine, respectively. Complete data sets can be found as Supplementary Figure 2. The effects of the cytostatic drugs on anti-IgM induced signaling were subsequently investigated (Figure 7).

The first cytostatic drug examined was fludarabine (Figure 7A). Anti-IgM induced signaling in M-CLL139 was reduced for Akt ($pSer^{473}$), p44/42 MAPK ($pThr^{202}/Tyr^{204}$), MAPKAPK-2 ($pThr^{334}$) and p38 MAPK ($pThr^{180}/Tyr^{182}$) relative to the average of healthy B cells after 3 min stimulation (Figure 7A, black bars). The anti-IgM induced signaling in UM-CLL135 and UM-CLL150 was increased for Akt ($pSer^{473}$) and p44/42 MAPK ($pThr^{202}/Tyr^{204}$), as well as for MEK1 ($pSer^{298}$) in UM-CLL150 (Figure 7A, black bars). Treatment with fludarabine did not significantly affect anti-IgM induced signaling in M-CLL139 (Figure 7A, grey bars). However, a slight increase in Akt ($pSer^{473}$), p44/42 MAPK ($pThr^{202}/Tyr^{204}$), MAPKAPK-2 ($pThr^{334}$) and p38 MAPK ($pThr^{180}/Tyr^{182}$) was observed in UM-CLL135 and UM-CLL150 after fludarabine treatment, as well as in MEK1 ($pSer^{298}$) in UM-CLL150 (Figure 7A, grey bars).

Next, the effect of doxorubicin on anti-IgM induced cell signaling was examined (Figure 7B). For UM-CLL135 and UM-CLL150, the phosphorylation levels were reduced for BLNK ($pTyr^{84}$) and Btk ($pTyr^{551}$) & Itk ($pTyr^{511}$) relative to the average of healthy B cells (Figure 7B, black bars). As observed after fludarabine treatment, doxorubicin also induced a small increase in Akt ($pSer^{473}$) and p44/42 MAPK ($pThr^{202}/Tyr^{204}$) in UM-CLL135 and UM-CLL150 (Figure 7B, grey bars). Interestingly, BLNK ($pTyr^{84}$) and p38 MAPK ($pThr^{180}/Tyr^{182}$) were specifically increased in the healthy B cells after doxorubicin treatment (Figure 7B, grey bars). Btk ($pTyr^{551}$) & Itk ($pTyr^{511}$) showed a small increase in the phosphorylation in both healthy and UM-CLL135 cells upon doxorubicin treatment, but note that the overall signal is very low (Figure 7B). For MEK1 ($pSer^{298}$), the signaling was somewhat enhanced in UM-CLL150 after treatment with doxorubicin and clearly induced relative to healthy controls (Figure 7B).

The last cytostatic drug examined was vincristine (Figure 7C). In M-CLL125, the signaling was observed to be similar for Akt ($pSer^{473}$) and impaired for Btk ($pTyr^{551}$) & Itk ($pTyr^{511}$) and SYK ($pTyr^{525/526}$) relative to healthy control cells (Figure 7C, black bars). The phosphorylation of Btk ($pTyr^{551}$) & Itk ($pTyr^{511}$) was impaired in both untreated UM-CLL135 and UM-CLL150 while SYK ($pTyr^{525/526}$) was unaffected in UM-CLL135 and reduced in UM-

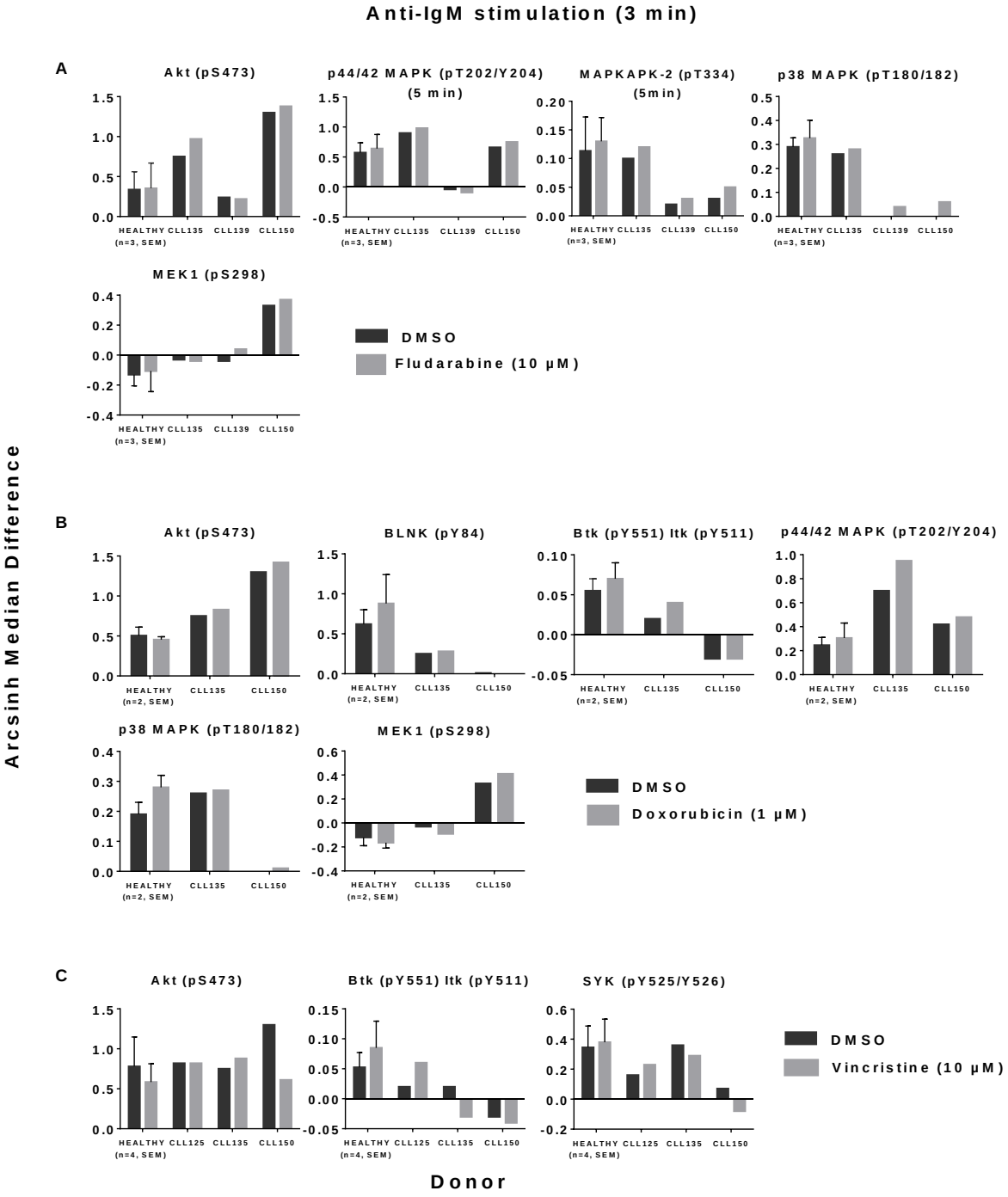

Figure 7. Effect of fludarabine, doxorubicin and vincristine on anti-IgM stimulated B cells. A) B cells from healthy donors (mean + SEM, n=3) and UM-CLL135, M-CLL139 and UM-CLL150 were incubated with fludarabine (10 µM) for 20 min, before stimulation with anti-IgM (1 µg/ml) for 3 min (unless otherwise indicated), and then processed and analysed as described in Figure 5. **B)** The experiments were performed as in A) on B cells from healthy donors (mean + SEM, n=2) and UM-CLL135 and UM-CLL150, but with doxorubicin (1 µM) instead of fludarabine. **C)** The experiments were performed as in B) on B cells from healthy donors (mean + SEM, n=4) and M-CLL125 UM-CLL135, UM-CLL150, but with vincristine (10 µM) instead of fludarabine.

CLL150, all relative to healthy control cells (Figure 7C, black bars). Treatment with vincristine had only minor effects. The most pronounced effect was that vincristine blocked the increase of Akt (pSer^{473}) in UM-CLL150 compared to healthy controls (Figure 7C).

Generally, the signaling was, in agreement with previous reports, enhanced in UM-CLL cells compared to the average of healthy controls after anti-IgM stimulation. After treatment with fludarabine or doxorubicin, the signaling was enhanced further, especially in UM-CLL135.

4.4 Idelalisib reverses the effect of fludarabine on Akt signaling

Idelalisib is a PI3Kδ inhibitor used in the treatment of CLL. It was investigated if it could reverse the elevated phosphorylation of Akt (pSer^{473}) seen in UM-CLL135 after treatment with fludarabine (Figure 7A). To this end, B cells from UM-CLL135 were treated with fludarabine or idelalisib alone, or in combination (Figure 8). The working concentration of idelalisib was selected after a titration study (data not shown).

As shown in Figure 8, fludarabine induced enhanced phosphorylation of Akt (pSer^{473}) after anti-IgM stimulation, while idelalisib strongly inhibited Akt (pSer^{473}) (Figure 8). Cells treated with the combination of fludarabine and idelalisib showed a reduction in Akt (pSer^{473}) similar to cells treated with idelalisib alone (Figure 8). This shows that idelalisib potently reverses the effect of fludarabine on Akt (pSer^{473}) phosphorylation.

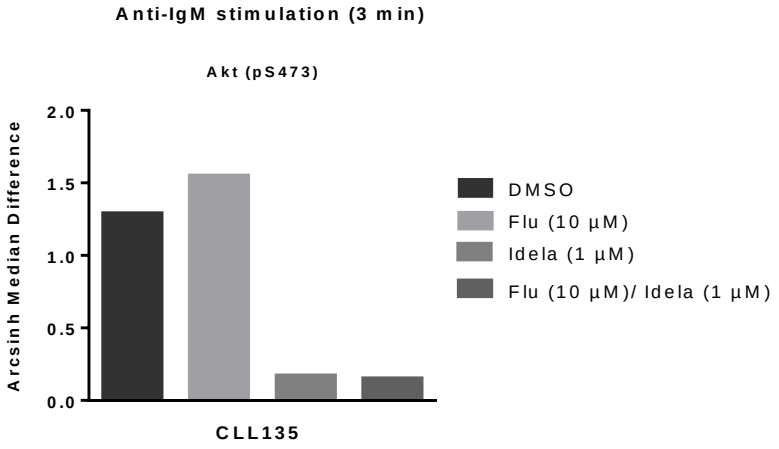

Figure 8. Effect of fludarabine and idelalisib on anti-IgM stimulated B cells. B cells from UM-CLL135 were incubated with fludarabine (10 µM), idelalisib (1 µM) or both for 20 min, followed by anti-IgM stimulation (1 µg/ml) for 3 min. The cells were processed and analysed as described in Figure 5. Flu; fludarabine, Idela; idelalisib.

4.5 Increased activation of Akt in M-CLL cells upon sCD40L stimulation

In addition to the BCR, the CLL cells also express the CD40 receptor. Stimulation of this receptor has been reported to synergize with the BCR signaling (Zenz et al. 2010). Based on this, it was of interest to map the signaling patterns elicited by sCD40L stimulation in CLL cells compared to healthy B cells. To this end, healthy B cells and M-CLL142 cells were stimulated with sCD40L (400 ng/ml) for both short (1-30 min) (Figure 9) and long (3-24 h) (Supplementary Figure 3) time periods.

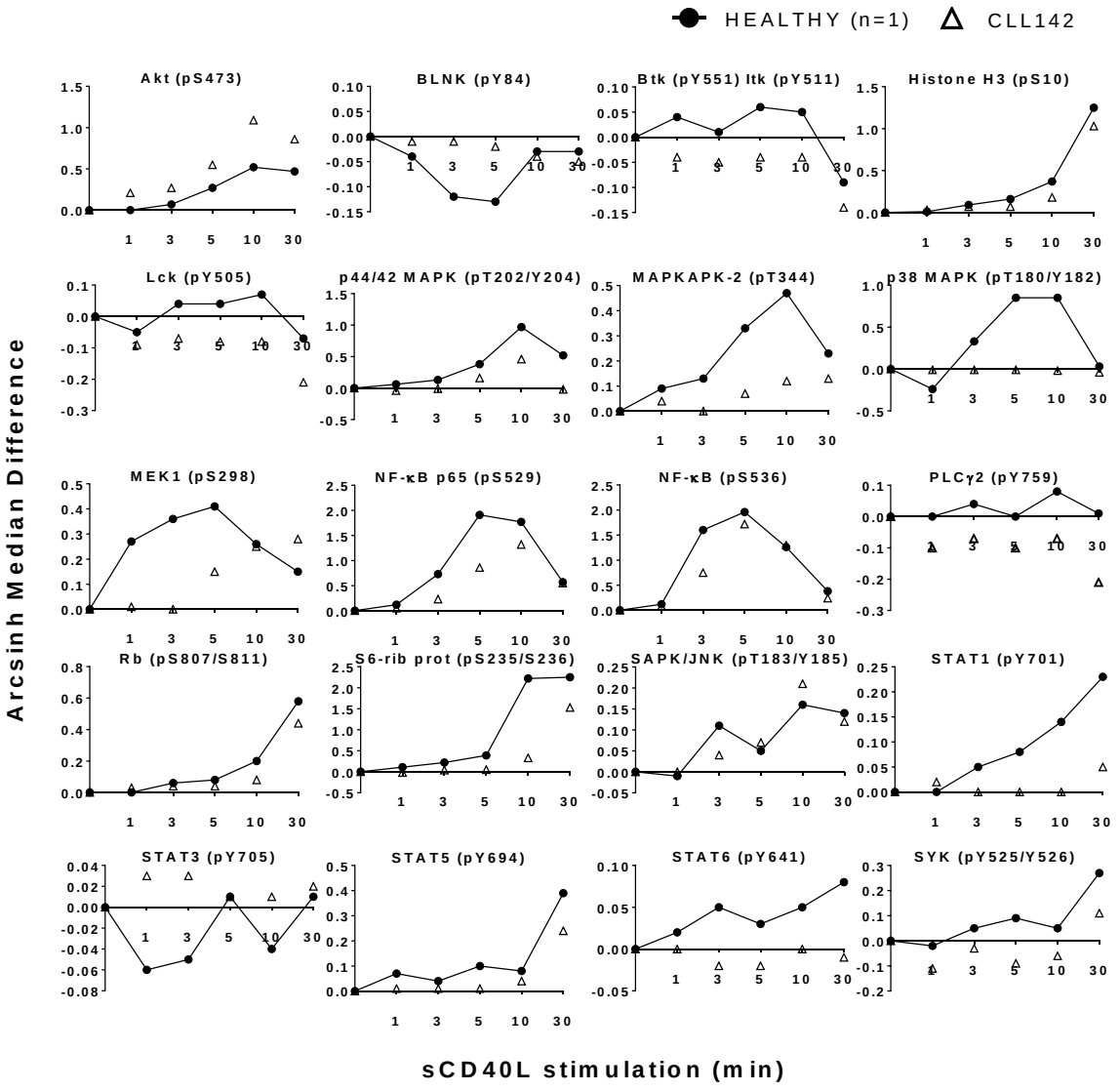

Figure 9. sCD40L induced signaling in B cells from healthy donors and CLL patients. B cells from healthy donor (n=1) and M-CLL142 were treated as in Figure 5, but with sCD40L (400 ng/ml) instead of anti-IgM.

M-CLL142 cells stimulated with sCD40L for up to 30 min elicited reduced signaling relative to healthy control cells for most of the parameters monitored (Figure 9). However, Akt (pSer^{473}) was clearly elevated in M-CLL142. This effect was lost after long stimulation (3-24 h, see Supplementary Figure 3), but here the overall signal amplitude was much lower as well. Reduced signal amplitudes were observed for several of the parameters after the long time course, resulting in few conclusive signaling differences between healthy donor and M-CLL142 (Supplementary Figure 3). Note that this experiment was performed on one healthy donor and one CLL patient only. sCD40L-induced signaling was best observed after a short time course, and M-CLL142 was hyporesponsive relative to the healthy donor for most of the parameters.

4.6 Cytostatic drugs enhance sCD40L induced signaling

Cells were next treated with fludarabine, doxorubicin or vincristine to assess the effect of these drugs on sCD40L induced signaling (Figure 10).

The first cytostatic drug examined to assess the effect on the sCD40L induced signaling was vincristine. As shown in Figure 10A-B, vincristine treatment altered the sCD40L induced signaling after both 5 min and 3 h for certain parameters. After 5 min stimulation, the phosphorylation of p44/42 MAPK (pThr^{202}/Tyr^{204}), MAPKAPK-2 (pThr^{334}) and SAPK/JNK (pThr^{183}/Tyr^{185}) in M-CLL142 was enhanced, relative to the internal control (Figure 10A, grey bars compared to black bars), while in healthy B cells, the phosphorylation level of p44/42 MAPK (pThr^{202}/Tyr^{204}) and MAPKAPK-2 (pThr^{334}) was suppressed after treatment (Figure 10A, grey bars). For untreated M-CLL142 relative to untreated healthy B cells, the phosphorylation of p44/42 MAPK (pThr^{202}/Tyr^{204}) and MAPKAPK-2 (pThr^{334}) was reduced (Figure 10A, black bars). After 3 h sCD40L stimulation, vincristine enhanced the phosphorylation level of all the parameters shown for both healthy B cells and M-CLL142, except for Akt (pSer^{473}) and p44/42 MAPK (pThr^{202}/Tyr^{204}) in healthy B cells (Figure 10 B, grey bars).

Next, the effect of fludarabine on sCD40L induced cell signaling was examined (Figure 10C). After 3 h sCD40L stimulation and drug treatment, the phosphorylation levels were enhanced for Akt (pSer^{473}) in M-CLL142 and for Histone H3 (pSer^{10}) and p44/42 MAPK (pThr^{202}/Tyr^{204}) in both healthy and M-CLL142 cells (Figure 10C, grey bars).

The last cytostatic drug examined was doxorubicin (Figure 10D). Doxorubicin induced its strongest relative effect on Btk (pTyr^{551}) & Itk (pTyr^{511}) in M-CLL142 cells after treatment

(Figure 10 D, grey bars). For the other parameters shown, doxorubicin enhanced the phosphorylation levels in M-CLL142, while healthy B cells responded with reduced phosphorylation for all parameters shown except Histone H3 (pSer^{10}), p44/42 MAPK

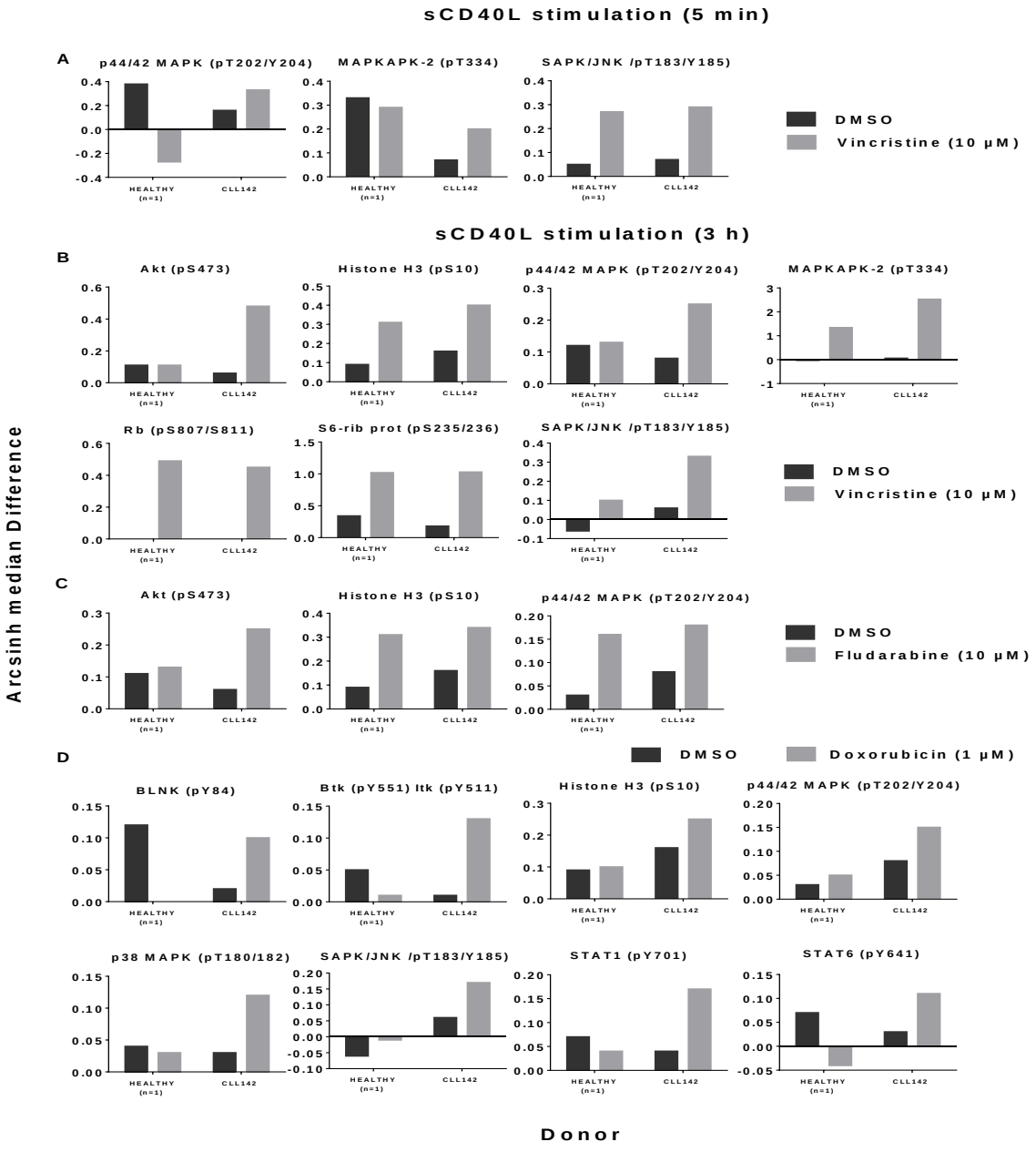

Figure 10 Effect of fludarabine, doxorubicin and vincristine on sCD40L stimulated B cells. A) B cells from healthy donor (n=1) and M-CLL142 were incubated with vincristine (10 µM) for 20 min, before stimulation with sCD40L (400 ng/ml) for 5 min. The cells were then processed and analysed as described in Figure 5. **B)** The experiment was performed as in A), but with 3 hours stimulation instead of 5 min. **C)-D)** The experiments were performed as in B), but with fludarabine (10 µM) and doxorubicin (1 µM) respectively, instead of vincrisitne.

(pThr^{202}/Tyr^{204}) and SAPK/JNK (pThr^{183}/Tyr^{185}). Note that the signaling amplitude for these parameters is relatively low. The results shown in Figure 10 are based on data from one healthy donor and one CLL patient. Overall, vincristine, fludarabine and doxorubicin induced phosphorylation of several signaling molecules in M-CLL142 after sCD40L stimulation.

4.7 Fludarabine inhibits STAT1 signaling after IFNγ stimulation

Since fludarabine has been reported to be a STAT1 inhibitor (Frank et al. 1999), it was of interest to assess the effect of this drug on the JAK/STAT pathway. To this end, the CD38 surface expression was used as readout since IFNγ has been reported to increase CD38 expression through the JAK/STAT pathway (Burgler et al. 2015). In parallel, cells were co-stimulated with CD40L expressing fibroblasts to provide anti-apoptotic stimuli and thereby allow the cells to survive during long-time IFNγ stimulation *in vitro* (Zenz et al. 2010) (Figure 11).

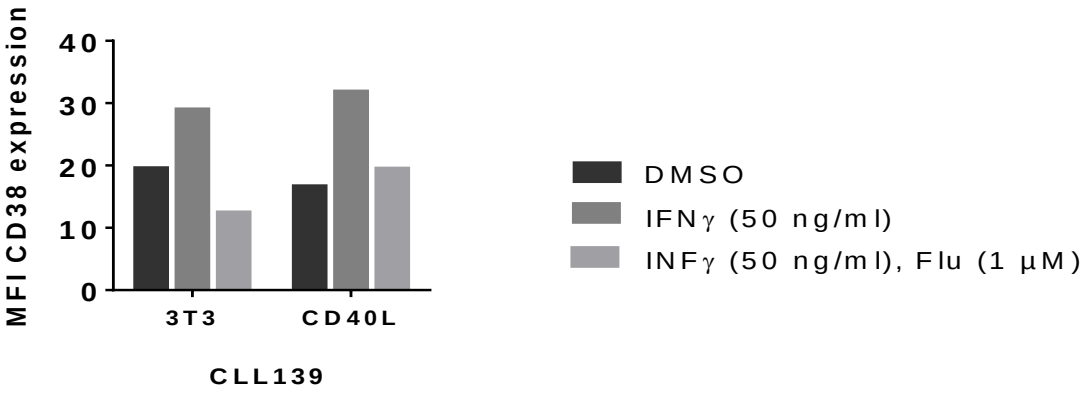

Figure 11. Effect of fludarabine on CD38 expression in CD40L and INFγ stimulated M-CLL139 cells. B cells from M-CLL139 were stimulated with CD40L transfected or unstransfected fibroblasts (NIH-3T3) in the presence or absence of IFNγ (50 ng/ml) and fludarabine (1 µM) for two days. The cells were then surface stained with anti-CD5, -CD19, -CD40 and -CD38 antibodies. The cells were analysed by flow cytometry and the data were processed in FlowJo. The median fluorescence intensity (MFI) for CD38 expression is shown. Flu; fludarabine.

IFNγ stimulation increased the CD38 surface expression compared to the unstimulated control (DMSO), both in the presence and absence of CD40L stimulation (Figure 11, dark grey bars). After fludarabine treatment, this effect was reversed, slightly more pronounced in the absence of CD40L stimulation (Figure 11, light grey bars). In summary, this result suggests that fludarabine inhibits STAT1 activation after IFNγ stimulation.

5 Discussion

In the present study, the effects of different stimuli and cytostatic drugs on signaling in B cells from healthy donors and CLL patients were investigated. Notably, the basal phosphorylation levels of BLNK (pTyr^{84}), Btk (pTyr^{551}) & Itk (pTyr^{511}), p38 MAPK (pThr^{180}/Tyr^{182}) and S6-Ribosomal protein (pSer$^{235/236}$) were all reduced in untreated CLL cells relative to untreated healthy B cells as well as in fludarabine treated cells. As shown, suppressed phosphorylation of these proteins were also observed in CLL cells treated with doxorubicin and vincristine, although these effects were not significant, possibly due to few patient samples examined. Therefore further analyses should be performed to investigate whether the observed differences are significant. Vincristine appeared to drug reverse the reduced basal phosphorylation level observed in untreated CLL cells relative to healthy controls. This suggests that one effect of this drug could be to normalize the impaired signaling in CLL cells. This should be investigated in more depth. Furthermore, presence of fludarabine reduced the basal level of SYK (pTyr^{352}) in CLL cells. It was recently shown that SYK inhibitors reduce proliferation of CLL cells (Parente-Ribes et al. 2016), and such inhibitors are undergoing clinical trials for use in the treatment of CLL. Knowing that SYK is involved in processes which promote growth and block apoptosis in B cells (Mocsai et al. 2010), this could be considered a positive side-effect of fludarabine.

A previous study on signaling in CLL cells (Blix et al. 2012) reported significantly higher basal phosphorylation levels of PLCγ (pTyr^{759}), p44/42 MAPK (pThr^{202}/Tyr^{204}), p38 MAPK (pThr^{180}/Tyr^{182}), NF-κB p65 (pSer^{529}), STAT5 (pTyr^{694}) and STAT6 (pTyr^{641}) in these cells compared to healthy B cells. In the present study, similar elevations in phosphorylation were not observed. In agreement with the data presented here, however, no significant change in SYK phosphorylation was observed by Blix et al., although the analysed phosphopitope differs between the studies (Blix et al. 2012). The inconsistence between the two studies may possibly be due to the different experimental approaches. In the study by Blix et al. the signaling patterns were characterized on thawed cells after 30 min incubation in medium. Here the cells were left over-night in medium before the signaling patterns were determined. Another difference between the studies which may impact the signaling is the origin of the patient material. Herein samples from CLL patients were investigated, whereas Blix et al. included samples from both CLL and small lymphocytic lymphoma (SLL) patients (Blix et al. 2012). Although these diseases are

essentially the same, the cancer cells appear at different locations in the body (Dores et al. 2007). The samples in the present study were obtained from blood whereas Blix et al. collected tumor biopsies (Blix et al. 2012). In addition, the CLL patient populations in these two studies may vary with respect to disease stage according to the Rai and Binet staging systems.

Interestingly, a significant increase in the basal level of STAT3 ($pTyr^{705}$) phosphorylation in CLL cells relative to healthy B cells was observed. Constitutive activation of STAT3 has been reported to be associated with hematological malignancies (Siveen et al. 2014). Cancer cells with constitutive STAT3 activation have also been reported to have elevated levels of cell cycle regulating and anti-apoptotic proteins, leading to resistance to apoptosis (Siveen et al. 2014). These reports underscore the relevance of the findings in this thesis, which is also in accordance with the statement that CLL cells are anti-apoptotic (Watson et al. 2008).

As reported, the basal level of phosphorylation was significantly increased in SAPK/JNK ($pThr^{183}/Tyr^{185}$) in CLL patients after vincristine treatment. This is in line with a previous report where the effect of vincristine was examined on ovarian carcinoma cells BR and MCF-7 breast cancer cells (Wang et al. 1998). Wang et al. reported that the fold activation of SAPK/JNK increased in a dose-dependent manner after treatment with vincristine.

When anti-IgM induced signaling was investigated, an increase in Akt ($pSer^{473}$) was observed for the two UM-CLL samples included, UM-CLL150 and UM-CLL135. The most prominent effect was observed in UM-CLL150 which could be explained by the *TP53* mutation in this patient since Akt is inhibited downstream of TP53 (Gottlieb et al. 2002).

Sustained activation of Akt through BCR stimulation promotes CLL cell survival (Longo et al. 2008; Petlickovski et al. 2005), as well as chemoresistance (Hofbauer et al. 2010). Hofbauer et al. observed clear apoptosis in fludarabine-resistant CLL cells after treatment with AiX which serves as an Akt inhibitor. This indicates that Akt plays a central role in fludarabine resistance. Increased activation of Akt ($pSer^{473}$) observed in UM-CLL135 and UM-CLL150 may therefore be an indicator for fludarabine resistance and presents a possible drug target in these patients. Indeed, as observed, the PI3K inhibitor idelalisib potently reversed the effect of fludarabine on Akt ($pSer^{473}$) in UM-CLL135. Idelalisib could therefore be an effective drug in combination with fludarabine in Akt induced CLL cells. However, Akt can also be activated by other signaling proteins than PI3K (Hofbauer et al. 2010). In the report by Hofbauer et al., Akt ($pSer^{473}$) was phosphorylated by protein kinase Cβ (PKCβ), which is central in BCR signaling.

In these situations Akt inhibitors such as enzastaurin have been effective (Hofbauer et al. 2010).

As observed, fludarabine induced a small increase in p44/42 MAPK ($pThr^{202}/Tyr^{204}$) in UM-CLL135 and UM-CLL150 patient samples. This is in agreement with the results reported by Fernández-Calotti et al. (Fernandez-Calotti et al. 2006). They observed that fludarabine effectively induced phosphorylation of ERK (p44/42 MAPK) in monocytic cells, already two minutes after treatment. Furthermore, they observed that fludarabine induced activation of the transcription factor AP1 through activation of the Ras-Raf-MEK-ERK pathway in both monocytic and CLL cells, indicating induced ERK activation in CLL cells as well. A possible negative side-effect of fludarabine could subsequently be differentiation and migration of the CLL cells since AP1 contributes to up-regulation of genes involved in these events.

In contrast, enhanced p38 MAPK signaling is involved in proapoptotic events (Xia et al. 1995), suggesting that fludarabine has an apoptotic effect on UM-CLL135, UM-CLL150 and M-CLL139. Fludarabine also induced activation of MAPKAPK-2 ($pThr^{334}$), a protein downstream of p38 MAPK, underpinning the enhanced effect of fludarabine on p38 MAPK ($pThr^{180}/Tyr^{182}$). Importantly, in the patients where fludarabine induces increased activation of both ERK and p38 MAPK, it would be of interest to target the Ras-Raf-MEK-ERK pathway to see if this could enhance the apoptotic effect of fludarabine even further.

As demonstrated, doxorubicin enhanced the signaling of Akt ($pSer^{473}$) and p44/42 MAPK ($pThr^{202}/Tyr^{204}$) in UM-CLL cells relative to untreated controls. A previous study showed that inhibition of the PI3K-Akt-mTOR and Ras-Raf-MEK-ERK survival pathways enhanced the effect of doxorubicin on apoptosis in HL-60 Human promyelocytic leukemia cells (Zhou et al. 2010). It would therefore be of interest to examine the effect of PI3K-Akt-mTOR and Ras-Raf-MEK-ERK pathway inhibitors in combination with doxorubicin on CLL cells.

An increase in Akt ($pSer^{473}$) was observed in M-CLL142 relative to healthy control after up to 30 min of sCD40L stimulation. After longer stimulation, this effect was lost. This is in line with a previous study where the phosphorylation level of Akt ($pSer^{473}$) was enhanced after stimulation with molecules mimicking the microenvironment of CLL, including CD40L, IL-2 and IL-10 (Balakrishnan et al. 2015). A moderately increased signaling of Akt ($pSer^{473}$) was seen after 30 min of stimulation, while after 4h the levels of phosphorylation was suppressed even below the basal level. Interestingly, after 72 h, the phosphorylation level was up to 50 fold higher than the basal phosphorylation level (Balakrishnan et al. 2015). Based on this report, it would be

of interest to include a 72 h time-point.

Since the PI3K-Akt-mTOR and Ras-Raf-MEK-ERK pathway are associated with proliferation and differentiation, the increased activation of Akt ($pSer^{473}$) and p44/42 MAPK ($pThr^{202}/Tyr^{204}$) in M-CLL142 after SCD40L stimulation and treatment with fludarabine, doxorubicin and vincristine suggests another negative side-effect of these drugs. However, this experiment is only based on examination of cells from one healthy donors and one CLL patient, it should therefore be repeated,

IFNγ stimulation of CLL cells increase the expression of CD38 in CLL cells through the JAK/STAT pathway (Burgler et al. 2015). Increased CD38 expression is associated with survival and proliferation of CLL cells, and the JAK/STAT pathway is by Burgler et al. reported to be a potential target in therapy of CLL. As observed in the present study, fludarabine suppressed the expression of CD38, supporting that the JAK/STAT pathway is involved in CD38 expression and that this pathway is a potential target in CLL therapy.

To conclude, the work presented in this thesis has added to the mapping of basal, anti-IgM- and CD40L-induced signaling in CLL cells compared to healthy B cells by the use of phosphoflow cytometry analysis. Furthermore, it has provided important information on signaling induced by the cytostatic drugs fludarabine, doxorubicin and vincristine. The findings reported here will be of value in the following studies which ultimately aim to provide personalized treatment of CLL patients.

References

Balakrishnan, K., Peluso, M., Fu, M., Rosin, N. Y., Burger, J. A., Wierda, W. G., Keating, M. J., Faia, K., O'Brien, S., Kutok, J. L., et al. (2015). The phosphoinositide-3-kinase (PI3K)-delta and gamma inhibitor, IPI-145 (Duvelisib), overcomes signals from the PI3K/AKT/S6 pathway and promotes apoptosis in CLL. *Leukemia*, 29 (9): 1811-22.

Bazargan, A., Tam, C. S. & Keating, M. J. (2012). Predicting survival in chronic lymphocytic leukemia. *Expert Rev Anticancer Ther*, 12 (3): 393-403.

Bertacchini, J., Heidari, N., Mediani, L., Capitani, S., Shahjahani, M., Ahmadzadeh, A. & Saki, N. (2015). Targeting PI3K/AKT/mTOR network for treatment of leukemia. *Cell Mol Life Sci*, 72 (12): 2337-47.

Blix, E. S., Irish, J. M., Husebekk, A., Delabie, J., Forfang, L., Tierens, A. M., Myklebust, J. H. & Kolstad, A. (2012). Phospho-specific flow cytometry identifies aberrant signaling in indolent B-cell lymphoma. *BMC Cancer*, 12: 478.

Burgler, S., Gimeno, A., Parente-Ribes, A., Wang, D., Os, A., Devereux, S., Jebsen, P., Bogen, B., Tjonnfjord, G. E. & Munthe, L. A. (2015). Chronic lymphocytic leukemia cells express CD38 in response to Th1 cell-derived IFN-gamma by a T-bet-dependent mechanism. *J Immunol*, 194 (2): 827-35.

Chiorazzi, N., Rai, K. R. & Ferrarini, M. (2005). Chronic lymphocytic leukemia. *N Engl J Med*, 352 (8): 804-15.

Ciccone, M., Ferrajoli, A., Keating, M. J. & Calin, G. A. (2014). SnapShot: chronic lymphocytic leukemia. *Cancer Cell*, 26 (5): 770-770 e1.

Cooper, G. M. (2000). *The Cell, A Molecular Approch*. Sunderland (MA): Sinauer Associates.

Dal-Bo, M., Bertoni, F., Forconi, F., Zucchetto, A., Bomben, R., Marasca, R., Deaglio, S., Laurenti, L., Efremov, D. G., Gaidano, G., et al. (2009). Intrinsic and extrinsic factors influencing the clinical course of B-cell chronic lymphocytic leukemia: prognostic markers with pathogenetic relevance. *J Transl Med*, 7: 76.

Damle, R. N., Wasil, T., Fais, F., Ghiotto, F., Valetto, A., Allen, S. L., Buchbinder, A., Budman, D., Dittmar, K., Kolitz, J., et al. (1999). Ig V gene mutation status and CD38 expression as novel prognostic indicators in chronic lymphocytic leukemia. *Blood*, 94 (6): 1840-7.

Dighiero, G. & Hamblin, T. J. (2008). Chronic lymphocytic leukaemia. *Lancet*, 371 (9617): 1017-29.

Do, B., Mace, M. & Rexwinkle, A. (2016). Idelalisib for treatment of B-cell malignancies. *Am J Health Syst Pharm*, 73 (8): 547-55.

Dores, G. M., Anderson, W. F., Curtis, R. E., Landgren, O., Ostroumova, E., Bluhm, E. C., Rabkin, C. S., Devesa, S. S. & Linet, M. S. (2007). Chronic lymphocytic leukaemia and small lymphocytic lymphoma: overview of the descriptive epidemiology. *Br J Haematol*, 139 (5): 809-19.

Durig, J., Naschar, M., Schmucker, U., Renzing-Kohler, K., Holter, T., Huttmann, A. & Duhrsen, U. (2002). CD38 expression is an important prognostic marker in chronic lymphocytic leukaemia. *Leukemia*, 16 (1): 30-5.

Döhner, H., Stilgenbauer, S., Benner, A., Leupolt, E., Krober, A., Bullinger, L., Dohner, K., Bentz, M. & Lichter, P. (2000). Genomic aberrations and survival in chronic lymphocytic leukemia. *N Engl J Med*, 343 (26): 1910-6.

Fabbri, G. & Dalla-Favera, R. (2016). The molecular pathogenesis of chronic lymphocytic leukaemia. *Nat Rev Cancer*, 16 (3): 145-62.

Fernandez-Calotti, P., Gamberale, R., Costas, M., Sanchez Avalos, J., Geffner, J. & Giordano, M. (2006). Fludarabine induces pro-inflammatory activation of human monocytic cells through a MAPK/ERK pathway. *Int Immunopharmacol*, 6 (5): 715-23.

Fidias, P., Chabner, B. A. & Grossbard, M. L. (1996). Purine Analogs for the Treatment of Low-Grade Lymphoproliferative Disorders. *Oncologist*, 1 (3): 125-139.

Frank, D. A., Mahajan, S. & Ritz, J. (1999). Fludarabine-induced immunosuppression is associated with inhibition of STAT1 signaling. *Nat Med*, 5 (4): 444-7.

Furman, R. R., Sharman, J. P., Coutre, S. E., Cheson, B. D., Pagel, J. M., Hillmen, P., Barrientos, J. C., Zelenetz, A. D., Kipps, T. J., Flinn, I., et al. (2014). Idelalisib and rituximab in relapsed chronic lymphocytic leukemia. *N Engl J Med*, 370 (11): 997-1007.

Gidding, C. E., Kellie, S. J., Kamps, W. A. & de Graaf, S. S. (1999). Vincristine revisited. *Crit Rev Oncol Hematol*, 29 (3): 267-87.

Gottlieb, T. M., Leal, J. F., Seger, R., Taya, Y. & Oren, M. (2002). Cross-talk between Akt, p53 and Mdm2: possible implications for the regulation of apoptosis. *Oncogene*, 21 (8): 1299-303.

Hallek, M., Cheson, B. D., Catovsky, D., Caligaris-Cappio, F., Dighiero, G., Dohner, H., Hillmen, P., Keating, M. J., Montserrat, E., Rai, K. R., et al. (2008). Guidelines for the diagnosis and treatment of chronic lymphocytic leukemia: a report from the International Workshop on Chronic Lymphocytic Leukemia updating the National Cancer Institute-Working Group 1996 guidelines. *Blood*, 111 (12): 5446-56.

Hock, B. D., McKenzie, J. L., McArthur, L., Tansley, S., Taylor, K. G. & Fernyhough, L. J. (2010). CD38 as a prognostic marker in chronic lymphocytic leukaemia at a single New Zealand centre: patient survival in comparison to age- and sex-matched population data. *Intern Med J*, 40 (12): 842-9.

Hoellenriegel, J., Meadows, S. A., Sivina, M., Wierda, W. G., Kantarjian, H., Keating, M. J., Giese, N., O'Brien, S., Yu, A., Miller, L. L., et al. (2011). The phosphoinositide 3'-kinase delta inhibitor, CAL-101, inhibits B-cell receptor signaling and chemokine networks in chronic lymphocytic leukemia. *Blood*, 118 (13): 3603-12.

Hofbauer, S. W., Pinon, J. D., Brachtl, G., Haginger, L., Wang, W., Johrer, K., Tinhofer, I., Hartmann, T. N. & Greil, R. (2010). Modifying akt signaling in B-cell chronic lymphocytic leukemia cells. *Cancer Res*, 70 (18): 7336-44.

Hus, I. & Rolinski, J. (2015). Current concepts in diagnosis and treatment of chronic lymphocytic leukemia. *Contemp Oncol (Pozn)*, 19 (5): 361-7.

Irish, J. M., Myklebust, J. H., Alizadeh, A. A., Houot, R., Sharman, J. P., Czerwinski, D. K., Nolan, G. P. & Levy, R. (2010). B-cell signaling networks reveal a negative prognostic human lymphoma cell subset that emerges during tumor progression. *Proceedings of the National Academy of Sciences of the United States of America*, 107 (29): 12747-12754.

Krutzik, P. O. & Nolan, G. P. (2006). Fluorescent cell barcoding in flow cytometry allows high-throughput drug screening and signaling profiling. *Nat Methods*, 3 (5): 361-8.

Landskron, J. & Tasken, K. (2016). Phosphoprotein Detection by High-Throughput Flow Cytometry. *Methods Mol Biol*, 1355: 275-90.

Longo, P. G., Laurenti, L., Gobessi, S., Sica, S., Leone, G. & Efremov, D. G. (2008). The Akt/Mcl-1 pathway plays a prominent role in mediating antiapoptotic signals downstream of the B-cell receptor in chronic lymphocytic leukemia B cells. *Blood*, 111 (2): 846-55.

Macintyre, E. A. & Linch, D. C. (1988). Lymphocytosis: is it leukaemia and when to treat. *Postgrad Med J*, 64 (747): 42-7.

Mocsai, A., Ruland, J. & Tybulewicz, V. L. (2010). The SYK tyrosine kinase: a crucial player in diverse biological functions. *Nat Rev Immunol*, 10 (6): 387-402.

Parente-Ribes, A., Skanland, S. S., Burgler, S., Os, A., Wang, D., Bogen, B., Tjonnfjord, G. E., Tasken, K. & Munthe, L. A. (2016). Spleen tyrosine kinase inhibitors reduce CD40L-induced proliferation of chronic lymphocytic leukemia cells but not normal B cells. *Haematologica*, 101 (2): e59-62.

Petlickovski, A., Laurenti, L., Li, X., Marietti, S., Chiusolo, P., Sica, S., Leone, G. & Efremov, D. G. (2005). Sustained signaling through the B-cell receptor induces Mcl-1 and promotes survival of chronic lymphocytic leukemia B cells. *Blood*, 105 (12): 4820-7.

Pokharel, M. (2012). Leukemia: A Review Article. *International Journal of Advaced Reseach in Pharmaceutical & Bio Science*, 2 (3): 397-407.

Rawlings, J. S., Rosler, K. M. & Harrison, D. A. (2004). The JAK/STAT signaling pathway. *J Cell Sci*, 117 (Pt 8): 1281-3.

Rogne, M. & Tasken, K. (2013). Cell signalling analyses in the functional genomics era. *N Biotechnol*, 30 (3): 333-8.

Siveen, K. S., Sikka, S., Surana, R., Dai, X., Zhang, J., Kumar, A. P., Tan, B. K., Sethi, G. & Bishayee, A. (2014). Targeting the STAT3 signaling pathway in cancer: role of synthetic and natural inhibitors. *Biochim Biophys Acta*, 1845 (2): 136-54.

Skånland, S. S., Moltu, K., Berge, T., Aandahl, E. M. & Tasken, K. (2014). T-cell co-stimulation through the CD2 and CD28 co-receptors induces distinct signalling responses. *Biochemical Journal*, 460: 399-410.

Tacar, O., Sriamornsak, P. & Dass, C. R. (2013). Doxorubicin: an update on anticancer molecular action, toxicity and novel drug delivery systems. *J Pharm Pharmacol*, 65 (2): 157-70.

Tjønnfjord, G. E., Ly, B. E., Johannesen, T. B., Tierens, A., Beiske, K., Heim, S. & Jonsson, V. (2012). Chronic lymphocytic leukaemia in Norway--incidence and prognostic markers at diagnosis. *Tidsskr Nor Laegeforen*, 132 (18): 2056-9.

Van Bockstaele, F., Verhasselt, B. & Philippe, J. (2009). Prognostic markers in chronic lymphocytic leukemia: a comprehensive review. *Blood Rev*, 23 (1): 25-47.

Vilpo, J. A., Koski, T. & Vilpo, L. M. (2000). Selective toxicity of vincristine against chronic lymphocytic leukemia cells in vitro. *Eur J Haematol*, 65 (6): 370-8.

Wang, T. H., Wang, H. S., Ichijo, H., Giannakakou, P., Foster, J. S., Fojo, T. & Wimalasena, J. (1998). Microtubule-interfering agents activate c-Jun N-terminal kinase stress-activated protein kinase through both ras and apoptosis signal-regulating kinase pathways. *Journal of Biological Chemistry*, 273 (9): 4928-4936.

Watson, L., Wyld, P. & Catovsky, D. (2008). Disease burden of chronic lymphocytic leukaemia within the European Union. *European Journal of Haematology*, 81 (4): 253-258.

WHO. (2014). *CHRONIC LYMPHOCYTIC LEUKEMIA. Union for International Cancer Control 2014 Review of Cancer Medicines on the WHO List of Essential Medicines* World Health Organization. Available at: http://www.who.int/selection_medicines/committees/expert/20/applications/cancer/en/ (accessed: 20.04.2016).

Xia, Z., Dickens, M., Raingeaud, J., Davis, R. J. & Greenberg, M. E. (1995). Opposing effects of ERK and JNK-p38 MAP kinases on apoptosis. *Science*, 270 (5240): 1326-31.

Zenz, T., Mertens, D., Kuppers, R., Dohner, H. & Stilgenbauer, S. (2010). From pathogenesis to treatment of chronic lymphocytic leukaemia. *Nat Rev Cancer*, 10 (1): 37-50.

Zhong, Y., Byrd, J. C. & Dubovsky, J. A. (2014). The B-cell receptor pathway: a critical component of healthy and malignant immune biology. *Semin Hematol*, 51 (3): 206-18.

Zhou, L., Luan, H., Dong, X. & Li, Y. (2010). Activation of the PI3K/Akt and MAPK signaling pathways antagonizes adriamycin-induced HL-60 leukemia cell apoptosis. *Mol Med Rep*, 3 (4): 641-4.

Supplement

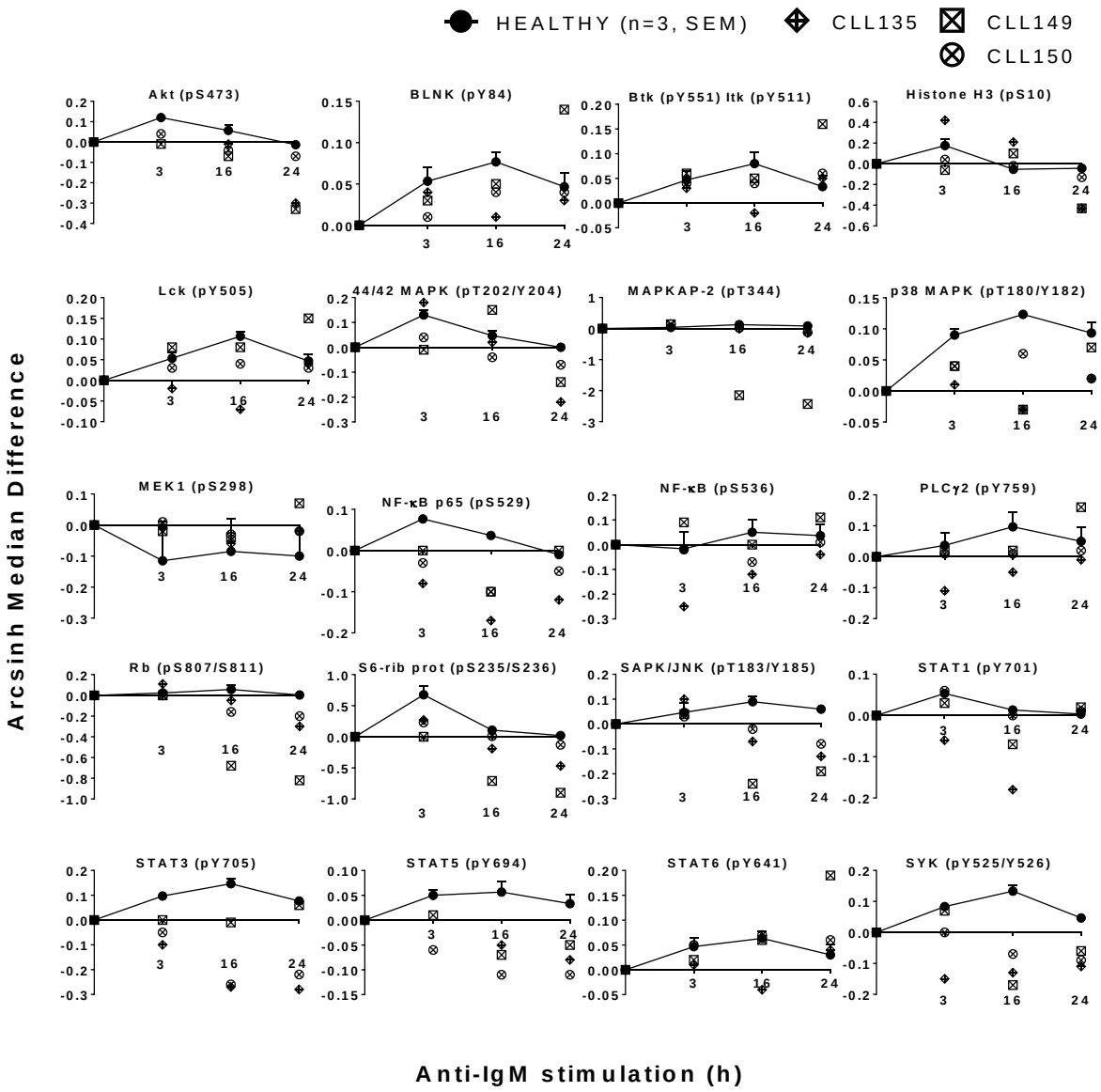

Supplementary Figure 1. Induced anti-IgM signaling in B cells from healthy donors and CLL patients. B cells from healthy donors (mean + SEM, n=3) and UM-CLL135, UM-CLL149 and UM-CLL150 were treated as in Figure 5.

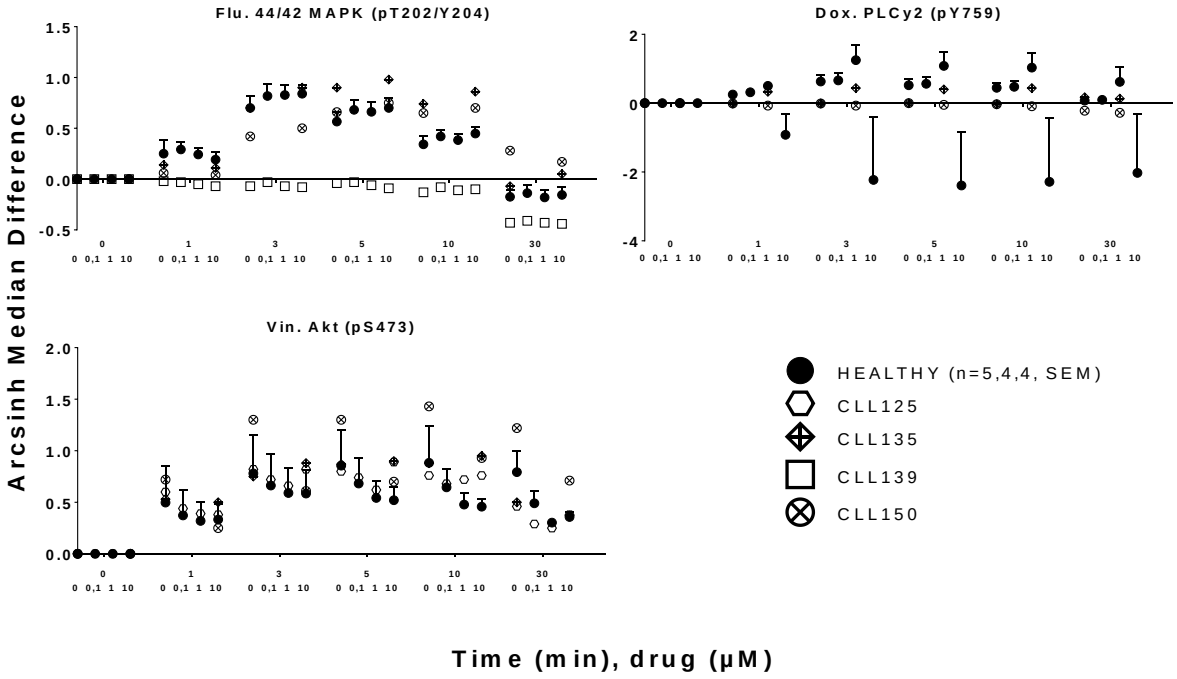

Supplementary Figure 2. Induced anti-IgM signaling in B cells from healthy donors and CLL patients treated with fludarabine, doxorubicin or vincristine. B cells from healthy donors (mean + SEM, n=4-5) and M-CLL125, UM-CLL135, M-CLL139 and UM-CLL150 were incubated with indicated concentrations of fludarabine, doxorubicin or vincristine for 20 min, before stimulation with anti-IgM (1 µg/ml) for the indicated time period. The cells were processed and analysed as described in Figure 5.

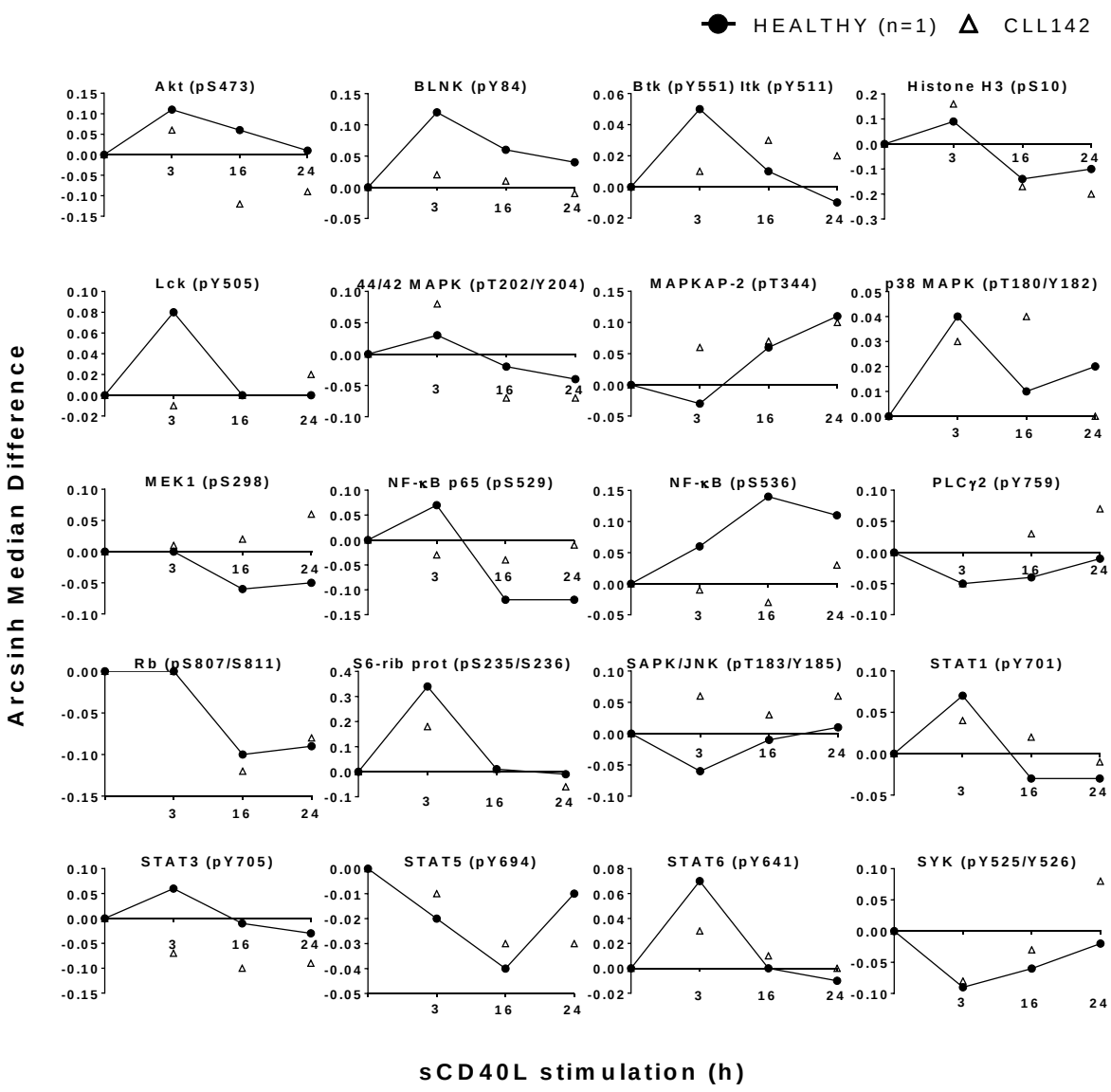

Supplementary Figure 3. Induced sCD40L signaling in B cells from healthy donors and CLL patients. B cells from healthy donors (n=1) and M-CLL142 were treated as in Figure 5, but with sCD40L (400 ng/ml) instead of anti-IgM.

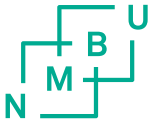

Norges miljø- og biovitenskapelig universitet
Noregs miljø- og biovitskapelege universitet
Norwegian University of Life Sciences

Postboks 5003
NO-1432 Ås
Norway